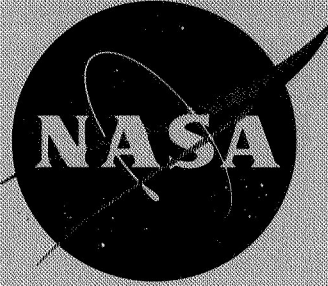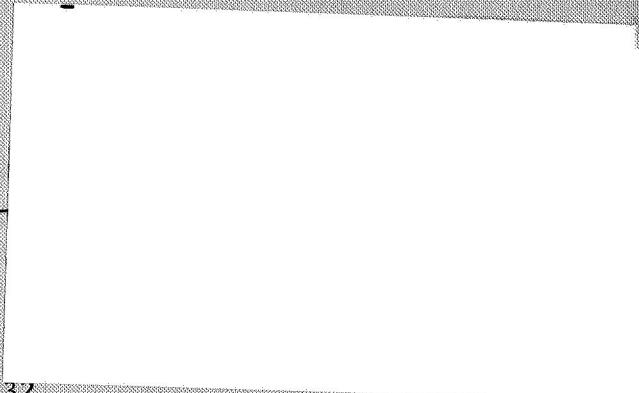CR 86068

NAS 12-32

GA-8238

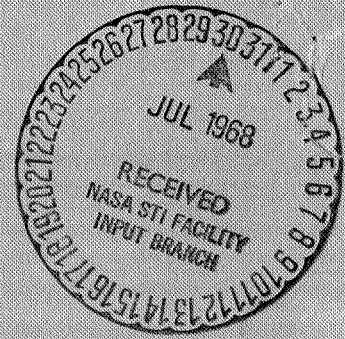RADIATION EFFECTS ON LASERS

by

D. M. J. Compton

FINAL REPORT

Contract No. NAS 12-32

Prepared for
National Aeronautics and Space Administration
Electronics Research Center
Cambridge, Massachusetts

November 1, 1967

Gulf General Atomic
Incorporated
P.O. Box 608, San Diego, California 92112

NOTICE

This report was prepared as an account of Government sponsored work. Neither the United States, nor the National Aeronautics and Space Administration (NASA), nor any person acting on behalf of NASA:

A.) Makes any warranty or representation, expressed or implied, with respect to the accuracy, completeness, or usefulness of the information contained in this report, or that the use of any information, apparatus, method, or process disclosed in this report may not infringe privately owned rights; or

B.) Assumes any liabilities with respect to the use of, or for damages resulting from the use of any information, apparatus, method or process disclosed in this report.

As used above, "person acting on behalf of NASA" includes any employee or contractor of NASA, or employee of such contractor, to the extent that such employee or contractor of NASA, or employee of such contractor prepares, disseminates, or provides access to, any information pursuant to his employment or contract with NASA, or his employment with such contractor.

RADIATION EFFECTS ON LASERS

by

D. M. J. Compton

FINAL REPORT

Contract No. NAS 12-32

During the period of this report, the
following "reportable items" as defined
by the article "Report of Technology"
evolved: None.

FOREWORD

This technical report, "Radiation Effects on Lasers" was prepared by Gulf General Atomic Incorporated, under Contract NAS 12-32 with NASA Electronics Research Center, Cambridge, Massachusetts. Research was carried out under the direction of Dr. D. M. J. Compton, the General Atomic Principal Investigator. The NASA Project Monitor was Mr. Charles Leigh. The research reported here was performed during the period from July 1, 1965 to October 1967.

CONTENTS

PRECEDING PAGE BLANK NOT FILMED.

FIGURES

I

INTRODUCTION

The work reported here is a continuation of a program started in July, 1965, to study the effects of space radiation on lasers, in order to develop the background knowledge needed for the possible application of laser systems in a space environment. A previous technical report[1] described the work performed in the period up to May 31, 1966, chiefly on analyzing the effects to be expected and on the development of instrumentation. In the present report, the effects of radiation are described for two main types of laser, GaAs laser diodes, and optically pumped lasers, such as ruby and Nd in various host materials. The mechanisms of the effects produced have been studied so that the results can be generalized with some confidence.

The results of the present program indicate that

1. neither type of laser is affected by doses and dose-rates of space radiation suitable for manned space flight.

2. for more severe environments, e.g., flights spending a large fraction of their time in the trapped radiation belts or with reasonably shielded on-board nuclear power, it is possible to select laser types which will be only minimally affected and whose performance can be restored by an annealing process. Shielding weights can also be calculated.

3. for very severe environments, e.g., near on-board nuclear power, it is at least possible to set certain guidelines relating to the effects to be expected.

The remaining components and interactions of a complete laser system now remain to be investigated. A start has been made in this contract period on measurements of space radiation effects on infrared detectors, and some consideration has been given to the damaging effects of the laser radiation itself and of interactions with other components of the space environment.

1

Since the publication of the previous report, little work on radiation effects on lasers has appeared in the literature. Johnson and Grow[2] have published a fuller report of their earlier work on ruby[3], and workers at NASA-Lewis have issued a brief report[4] on some effects of radiation on the Cr^{3+} ions in ruby. Recent work on GaAs diodes is reviewed in the following section.

II

RADIATION DAMAGE TO GaAs LASER DIODES

This section describes the progress made in evaluating and under-
standing the effects of radiation damage in GaAs laser diodes. Such effects
are of importance, not only in possible uses of lasers for communication,
but also for the numerous other uses of GaAs lasers and light-emitting
diodes in data handling and in such devices as high-isolation, optically
coupled, circuits.

2. 1   Previous Work on Radiation Effects on Diode Lasers and Electro-
        luminescent Devices

Relatively little work has been performed in this field. Measure-
ments on GaAs lasers have been made by Saji and Inuishi,[5] who briefly
reported some effects of Co^{60} γ-irradiations. Although their results are
fragmentary and inconclusive, they show a decrease of laser output after
irradiation that can be partially recovered by annealing at 120° - 200°C.
The emission was shifted slightly to shorter wavelengths. J. H. Doede,
et al,[6] report, in an abstract of a conference paper, fast neutron effects
on the threshold currents of $GaAs_{(1-x)}P_x$ p-n junction diode lasers. They
find that neutron bombardment gives a linear degradation of the threshold
current, and they attribute this to surface damage effects on the reflectivity
of the cavity ends.

Radiation effects on GaAs electroluminescent (EL) diodes have been
studied by several workers. Petree[7] measured the effects of fast neutron
irradiation on GaAs EL diodes and found a progressive destruction of the
luminescent output, beginning at a dose of 10^{12} neutrons/cm^2 and a reduc-
tion in the output to ~ 0.01 of the original value after a radiation dose of
$\sim 10^{14}$ neutrons/cm^2 (>10 keV). Millea and Aukerman[8] investigated the role
of diffusion current in the electroluminescence of GaAs diodes, and used
irradiation with 2 MeV electrons as a tool to change the minority carrier
lifetime. They found a reduction in intensity by about a factor of 10
after an irradiation with 3×10^{15} electrons/cm^2, and a dose depen-
dence consistent with a model predicting a decrease of intensity, at
constant current, proportional to $(dose)^{-3/2}$. In a later communication,[9]

3

the same authors report work on radiation damage by 2 MeV electrons to heavily doped GaAs diodes, in which both the current and emission intensity were measured. At low forward voltages, the current is greatly increased by a dose of $\sim 3 \times 10^{16}$ 2 MeV electrons/cm^2, while the electroluminescent output is only slightly decreased. The results are explained on a bandfilling model. Results are not given for high applied voltages and high forward currents, but it appears that diffusion current is important. Another paper by the same authors[10] treats the electroluminescent emission at wavelengths corresponding to energies substantially lower than the bandgap. While the near-bandgap emission intensity is proportional to current at high currents, the emission bands at longer wavelengths tend to saturate with increasing current. The near-bandgap emission was reduced in intensity by a factor of ~ 6 (at constant voltage) at 300°K by a dose of $\sim 2.8 \times 10^{15}$ 2 MeV electrons/cm^2, while the 1.0 eV band is much more sensitive, being reduced by a factor of 30 under similar conditions. Aukerman, Millea and McColl[11] also studied the diffusion lengths of electrons and holes in GaAs diodes, using 2 MeV electrons to inject carriers. In the course of the experiment they also found a reduction of diffusion length produced by the irradiation, corresponding to a decrease of carrier lifetime, with the reciprocal of the electron lifetime varying linearly with the radiation dose. In their paper, no measurement was made of the effects of irradiation on the intensity of optical emission. The work of these authors, using radiation damage as a tool to study the properties of GaAs p-n junctions, has also been recently summarized.[12]

A larger amount of work has been performed on the general topic of radiation damage in bulk GaAs. Aukerman and co-workers[13,14] have studied the effects of electron and reactor irradiations on the electrical properties of GaAs, and also annealing of the damage. Bauerlein[15] and Grimshaw and Banbury[16] have studied the threshold energy for production of displacement damage in GaAs by electron bombardment. The effects of electron and proton irradiation on luminescence have been studied by Loferski and Wu.[17] They used the luminescence produced by irradiation to study radiation damage. A threshold for radiation damage by electrons was measured. It was noted that proton bombardment would also produce luminescence, but no quantitative damage effects were reported. An anomalous infrared absorption is found in compound semiconductors such as GaAs when they are irradiated with fast neutrons. This is accounted for by McNichols and Ginell[18] in terms of a local phase change in spikes to a metallic-like state.

2.2   Apparatus and Techniques

To study the effects of radiation on GaAs lasers, the apparatus described in the previous technical report[1] was used. A cryostat is used to maintain the laser at liquid nitrogen temperatures when desired, and is furnished with thin windows of high-purity synthetic fused silica (Suprasil) to allow the laser radiation to escape. No significant optical absorption in the infrared is produced in this material by the irradiation to which it is exposed during a series of experiments. Thin Mylar windows allow for the entrance of the high-energy particulate radiation, and are replaced as necessary when radiation-induced cracking causes leaks. A coaxial cable feedthrough enables exciting current pulses to be supplied to the laser. The current in each pulse is measured with a Tektronix CT-2 current transformer and displayed on one beam of a dual-beam oscilloscope. The other beam is used to display the optical output, which is derived either from a high-current, infrared-sensitive, biplanar photodiode (ITT FW4000 SI), or from a photomultiplier tube (RCA 7102). The latter has only a limited dynamic range, since only small currents may be drawn; also, it does not have fast response, since a 10K load resistor is generally used to give an adequate signal; but the photomultiplier is useful when it is desired to study both spontaneous and stimulated emission in the same experiment. Neutral-density filters are inserted in the optical path when stimulated emission is measured, and removed when spontaneous emission is to be measured. The biplanar photodiode is too insensitive to make convenient measurements of the spontaneous emission.

Photographs are taken of the optical output of the diode at a number of different current levels, and the results are used to yield a plot of peak output power vs peak current in the pulse. Another method of obtaining such plots is presently being tested: peak-reading circuits are used to feed the outputs of the current and optical intensity channels into electrometers which, in turn, drive an X-Y recorder. The diode is then pulsed repetitively with the current being slowly increased. The recorder plots the optical output vs current.

Typical oscilloscope traces are shown in Fig. 1, and the plot of optical output vs peak current obtained is shown in Fig. 2. The plot shows an initial region of spontaneous emission, followed by a fairly sharp threshold to stimulated emission, where the output increases linearly with input current, followed by a saturation region. The last region is unusually severe in this plot, and it was selected to demonstrate this effect.

5

0.005 v/cm   0.02 v/cm   0.05 v/cm
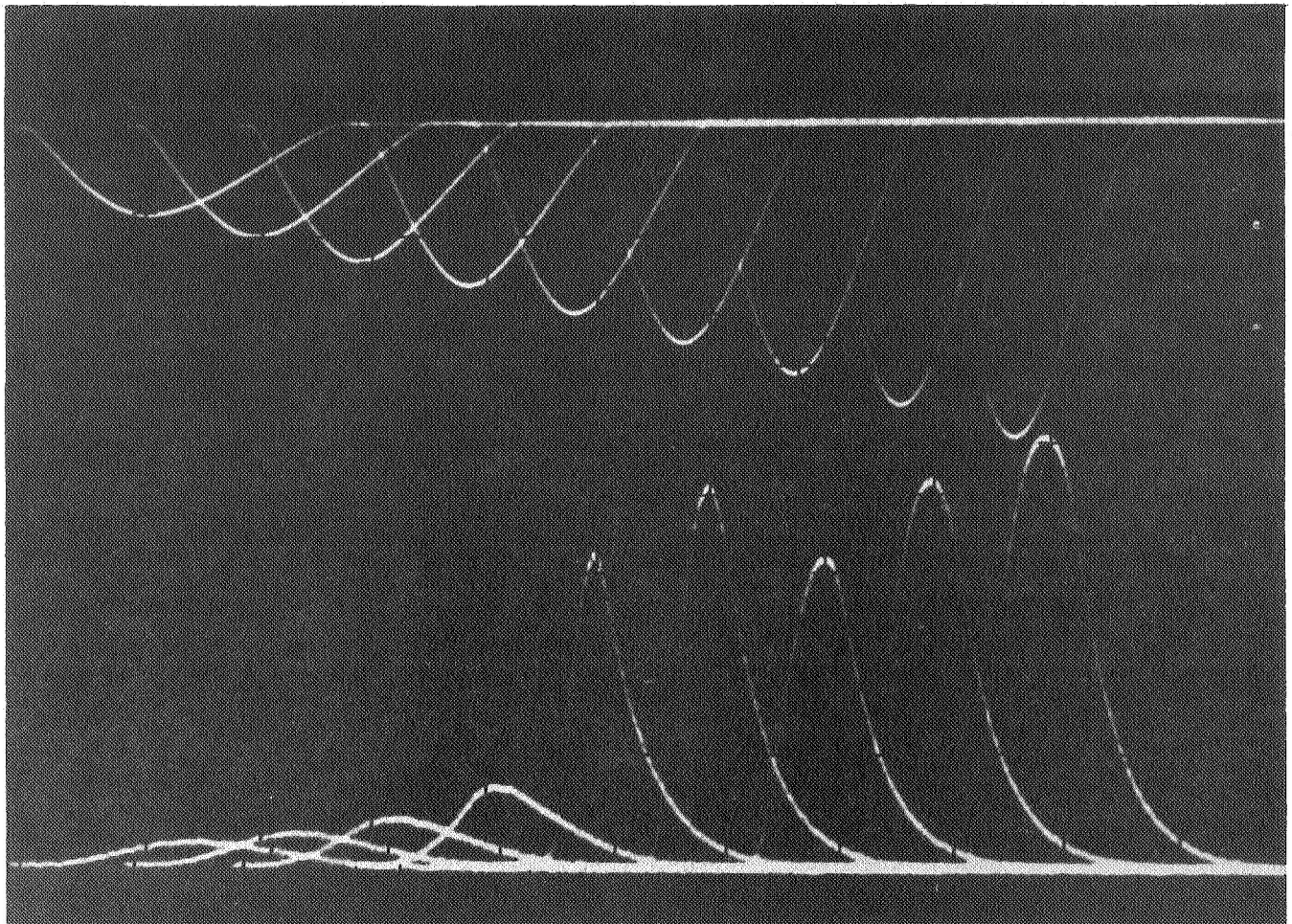
Upper Trace: Forward injection current, increasing from left to right;
            beginning at 0.7 amps and ending at 2.4 amps. Gain: 1 v/cm
            Sweep: 2 μsec/cm, from left to right.
Lower Trace: Laser optical output signal. Gain as shown.

Fig. 1a--Oscilloscope traces showing laser output and injection current for
        GE H1D1 diode at 77°K

0.05 v/cm | 0.1 v/cm
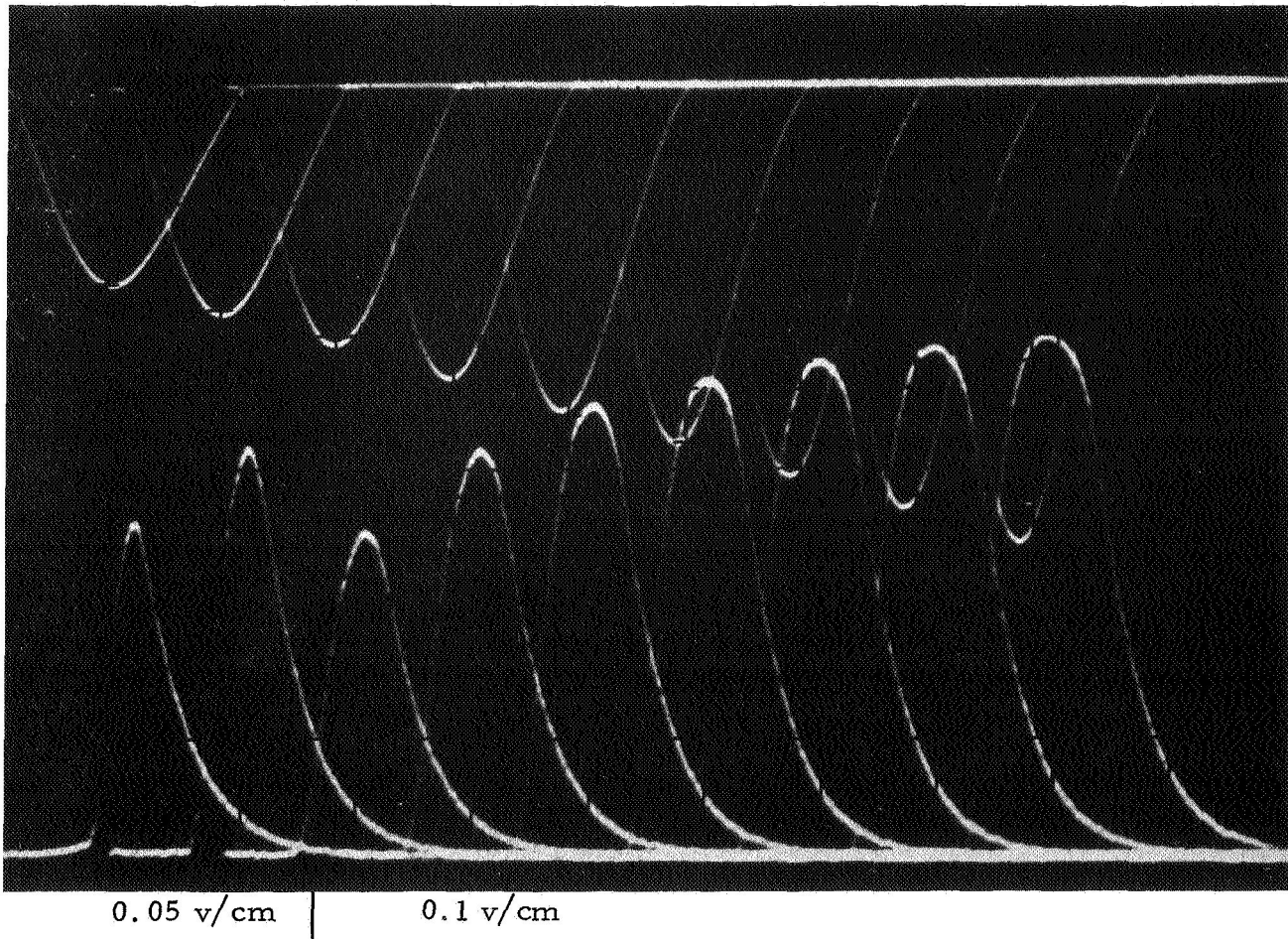
Upper Trace: Forward injection current, increasing from left to right, beginning at 1.7 amps and ending at 3.4 amps. Gain: 1 v/cm

Lower Trace: Laser optical output; gains as shown. Sweep 2 μsec/cm, right to left.

Fig. 1b--Oscilloscope traces showing laser output and injection current for GE H1D1 diode at 77°K.
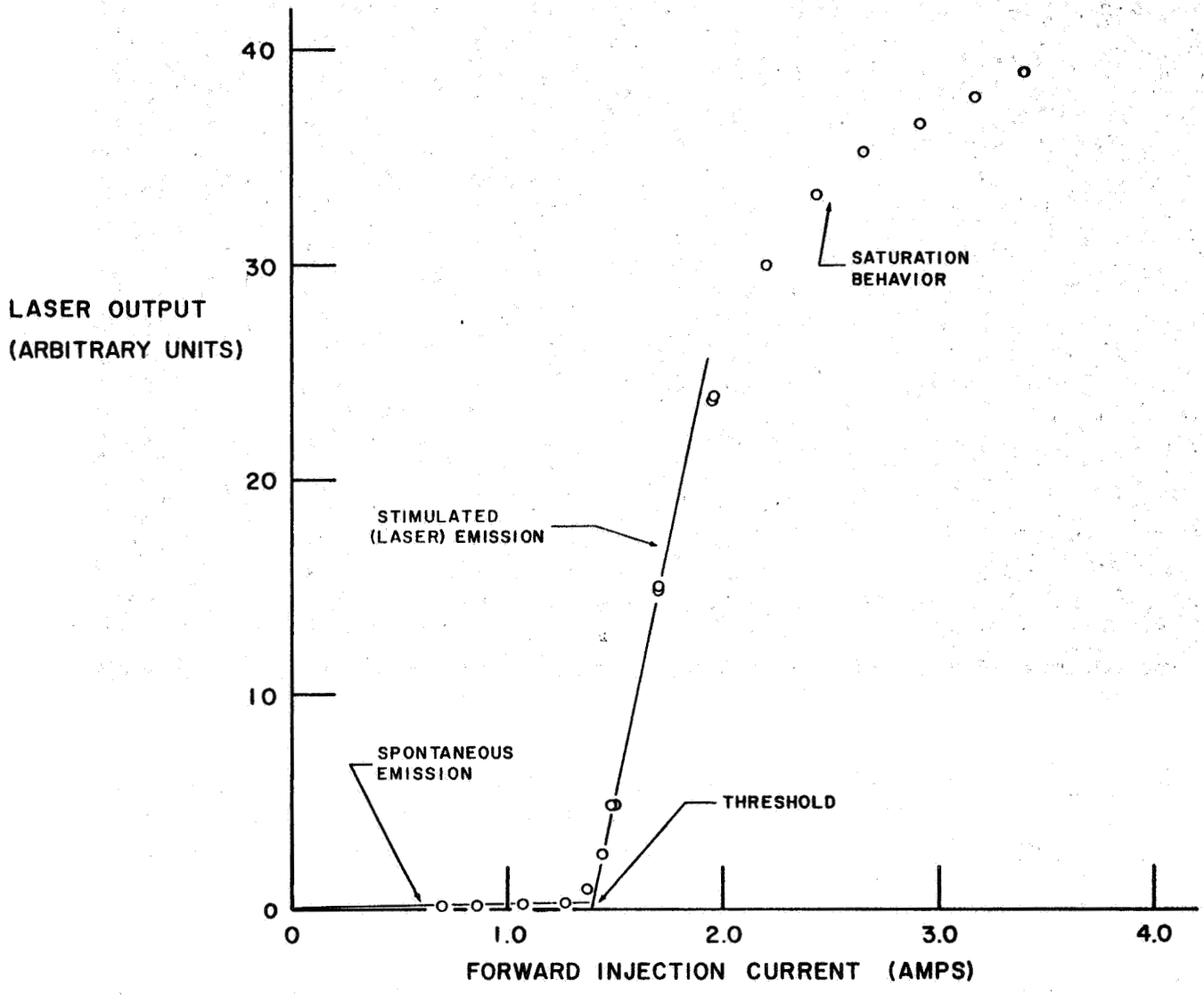
Fig. 2--Plot of laser output vs injection current showing spontaneous emission, stimulated emission, and saturation regions for GE H1D1 diode at 77°K

The current pulse width used was typically 1 - 2 μsec, although narrower pulses were used when desired. GaAs lasers are supplied on headers which have a cap with a window. To avoid possible confusing effects from coloration of this window by the irradiation[*], it was removed. On some types of laser the cap can be lifted off; on others it was machined off on a lathe. The removal of this cap was, however, the source of an unexpected problem. On cooling a diode to 77°K in the cryostat, the laser output was sometimes found to show a slow variation with time. This is attributed to the deposition, on the end faces of the laser, of layers of condensed material, probably water from small leaks in the cryostat. These act as anti-reflection coatings, and lower the output of the laser. This interpretation is based on a slow periodic variation of the laser output with time, thought to be due to the slow increase of thickness through integral numbers of quarter wavelengths, and on the absence of any effect on the spontaneous emission, from these diodes or on the laser emission from diodes with reflective coatings applied to the end faces (e. g. the Korad K-S1). The problem was overcome by improving the leak-tightness of the cryostat, and by avoiding long periods of standing at liquid nitrogen temperature.

2.3 General Description of Effects Found

A number of diode types were studied. Some initial measurements were made on Korad type K-S1 and Maser Optics DLP-4 diodes, but these showed generally poor laser characteristics. Most of the work was performed on GE H1D1 and RCA TA 2628 laser diodes, since these showed reasonably good laser characteristics and good reproducibility from unit to unit. Some preliminary measurements were made on $Ga(As_x P_{1-x})$ diodes, which emit in the red, but no significant understanding was gained.

The general features found for radiation damage to the output properties of a GaAs laser diode are shown in Fig. 3 for the case of a General Electric H1D1 unit operated in the pulsed mode at 77°K. The left-hand line is a plot of peak optical output intensity vs peak forward current, taken at 77°K before irradiation. The succeeding lines to the right correspond to increasing doses of electron irradiation at 77°K, but the effects

---

[*] The coloration of the window was later measured separately and found to be negligible in the 8000 - 9500 Å region for radiation doses sufficient to permanently destroy laser action in a GaAs diode.

9
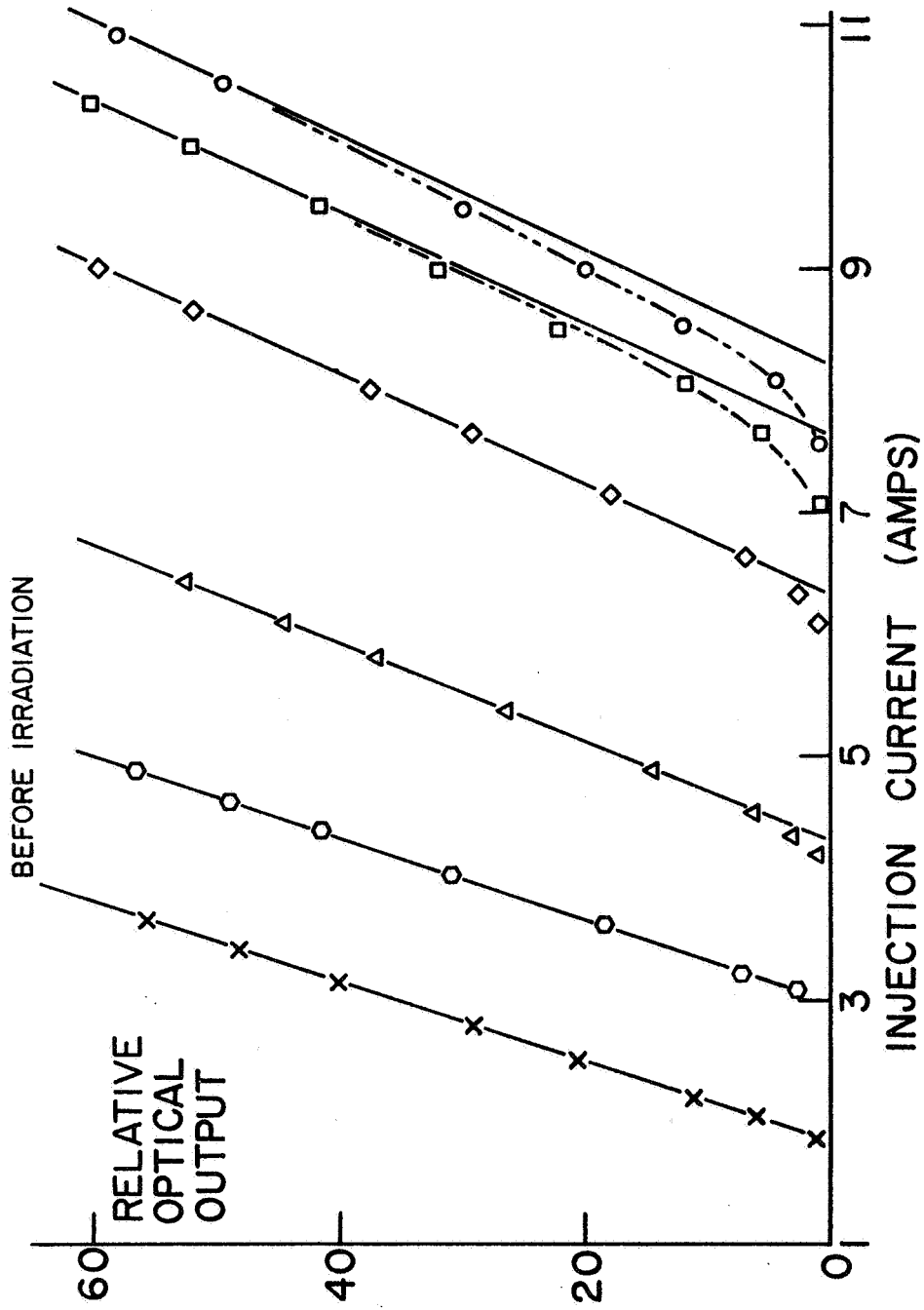
Fig. 3--General features of radiation damage to output of GE H1D1 diode measured at 77°K. Line at left is before irradiation. Increasing doses of radiation produce the succeeding lines to right, while annealing returns lines towards left.

can be reversed and the lines can be returned toward the left by an annealing procedure described below. The chief effect of irradiation is to change the threshold current. At higher doses, there is also a relatively small decrease in the slope of the output vs input curve, and a rounding-off of the curve near threshold, so that the threshold is no longer sharp.

The current-voltage characteristics of the diode were measured before and after irradiation. At low voltages and currents (up to a few ma) a Tektronix 575 transistor tester was used. At higher currents, corresponding to laser operation, the measurement is more difficult, since the current is applied in fast pulses. An attempt to measure the I-V characterestics by applying voltage probes to the diode gave signals that were difficult to interpret because of capacitive and charge-storage effects. An indication of current-voltage characteristics was thus obtained from the voltage used to charge the capacitor in the pulse generating circuit.

At low voltages (< 1 volt) the I-V characteristics are considerably changed, in the manner described by Aukerman et al,[12] the forward current being increased by the addition of a diffusion component. An extreme case is shown in Fig. 4. This figure shows the I-V characteristics of an RCA type TA 2628 diode before and after irradiation with 5.7×10^{14} 28 MeV electrons/cm^2, a dose which increases the threshold current at 77°K from 1.4 to 6.8 amps, but leaves the diode still able to give laser emission. At the higher voltages and currents needed to produce laser action, there is no significant change after irradiation.

The GE H1D1 diode is, however, less affected in its I-V characteristics than the RCA TA 2628. Figure 5 shows the low voltage I-V characteristics of a H1D1 diode after a dose of 1.6×10^{14} 30 MeV electrons/cm^2, sufficient to change the threshold from 1.5 to 4.2 amps. No change is caused in either the forward or reverse characteristics. The difference between the two types of diode is presumably related to a difference in doping level. For the H1D1 diode, there is again no change in I-V characteristics at high currents, as shown in Fig. 6.

The effects on laser threshold could be due to the irradiation producing either a decrease in the EL efficiency or an increase in the optical absorption in the active region of the diode. An equation for the current density at threshold in terms of these quantities is given by Nathan[19] as

$$j_t = \frac{8\pi e n_o^2 \nu^2 d \Delta \nu}{\eta c^2} \left[\frac{1}{\ell} \ln(1/R) + \alpha \right] , \qquad (1)$$

11
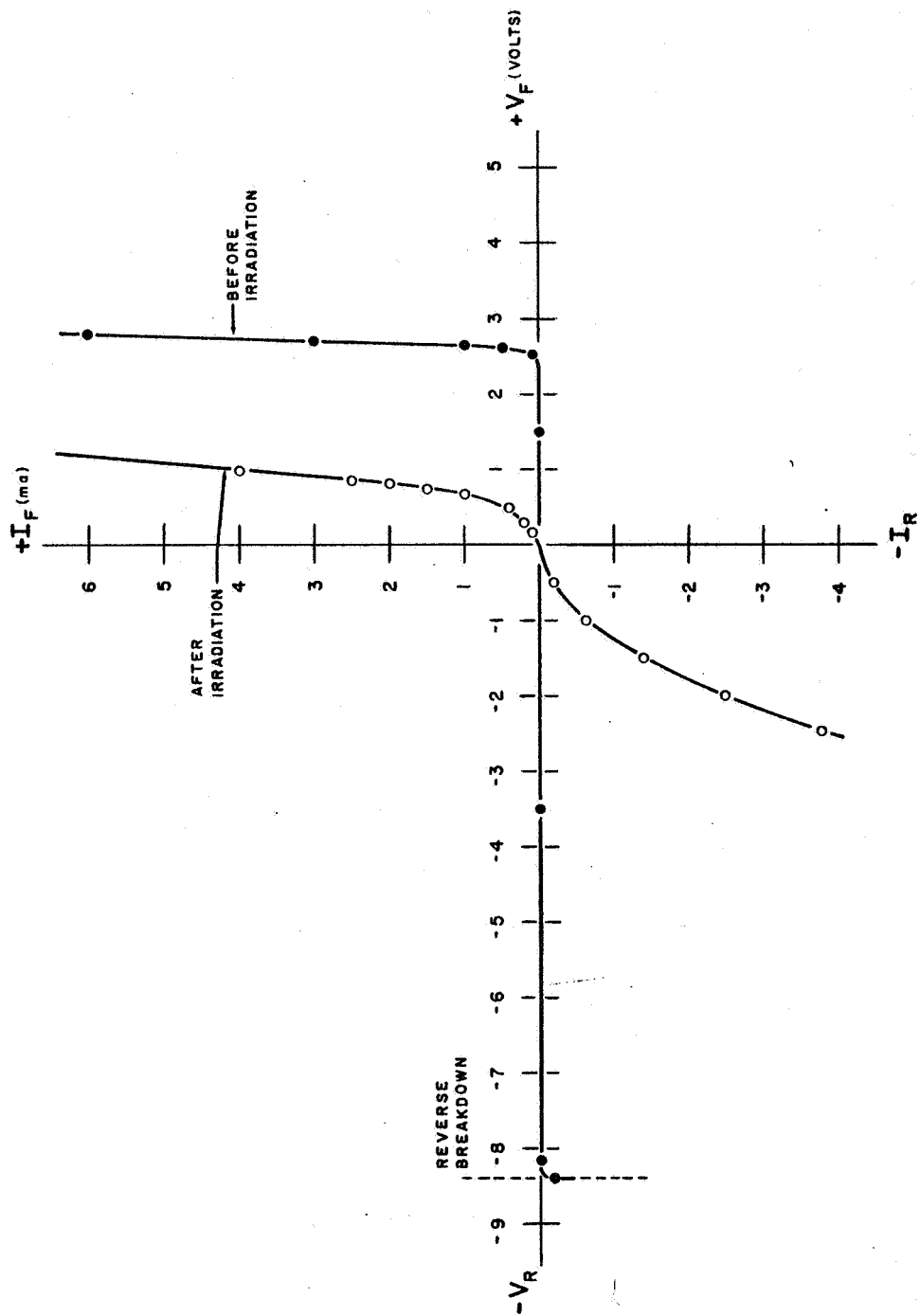
Fig. 4--Low-current forward I-V characteristics at 77°K of RCA TA 2628 diode before and after irradiation with 5.7 x 10^14 28 MeV electrons/cm², the threshold current at 77°K being changed from 1.4 to 6.8 amps.
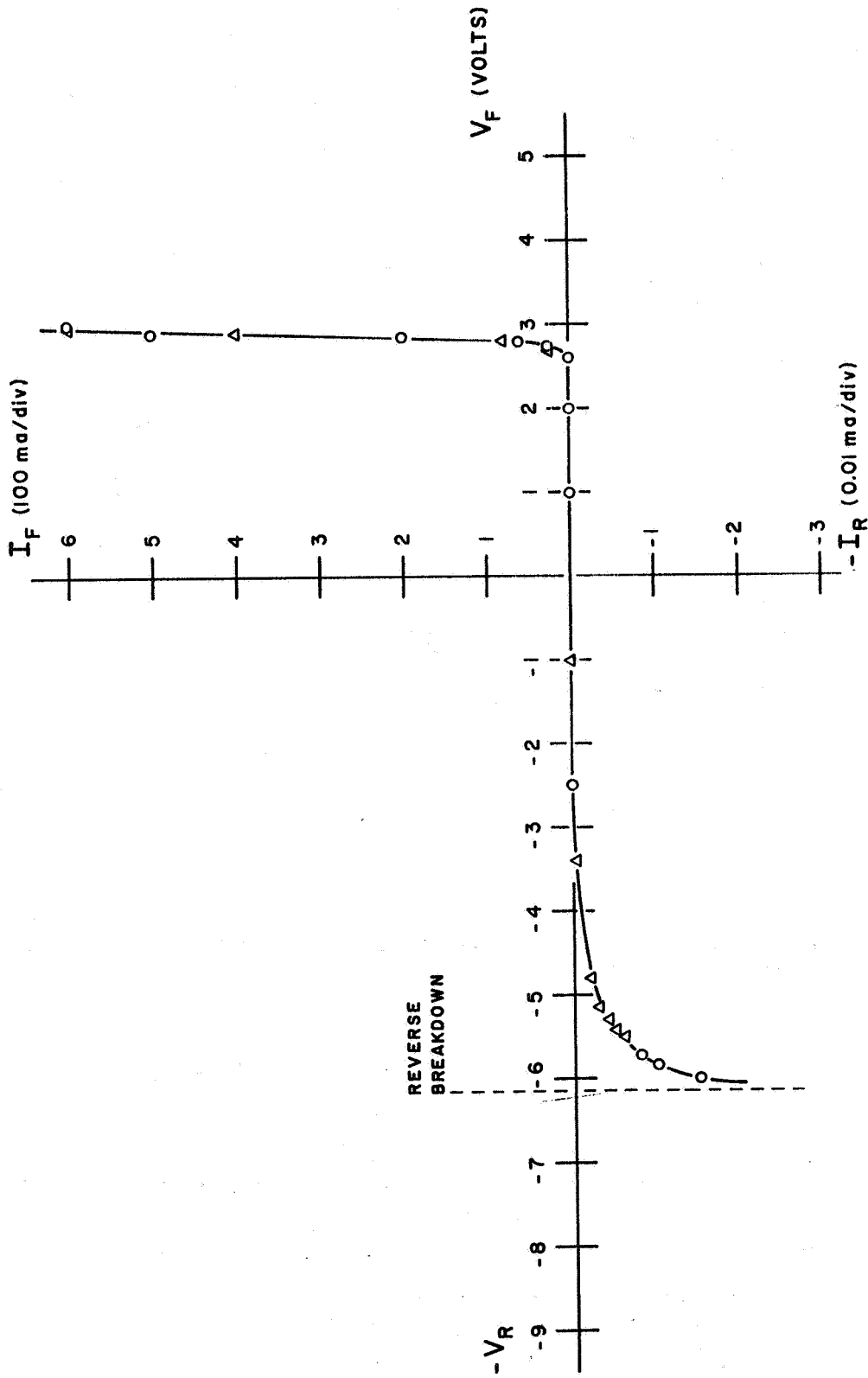
Fig. 5--Low current forward I-V characteristics of GE H1D1 diode taken at $77^{O}K$ on Tektronix 575 tester. $\triangle$ before and O after a dose of 1.6×10^{14} 30 MeV electrons/cm^2.
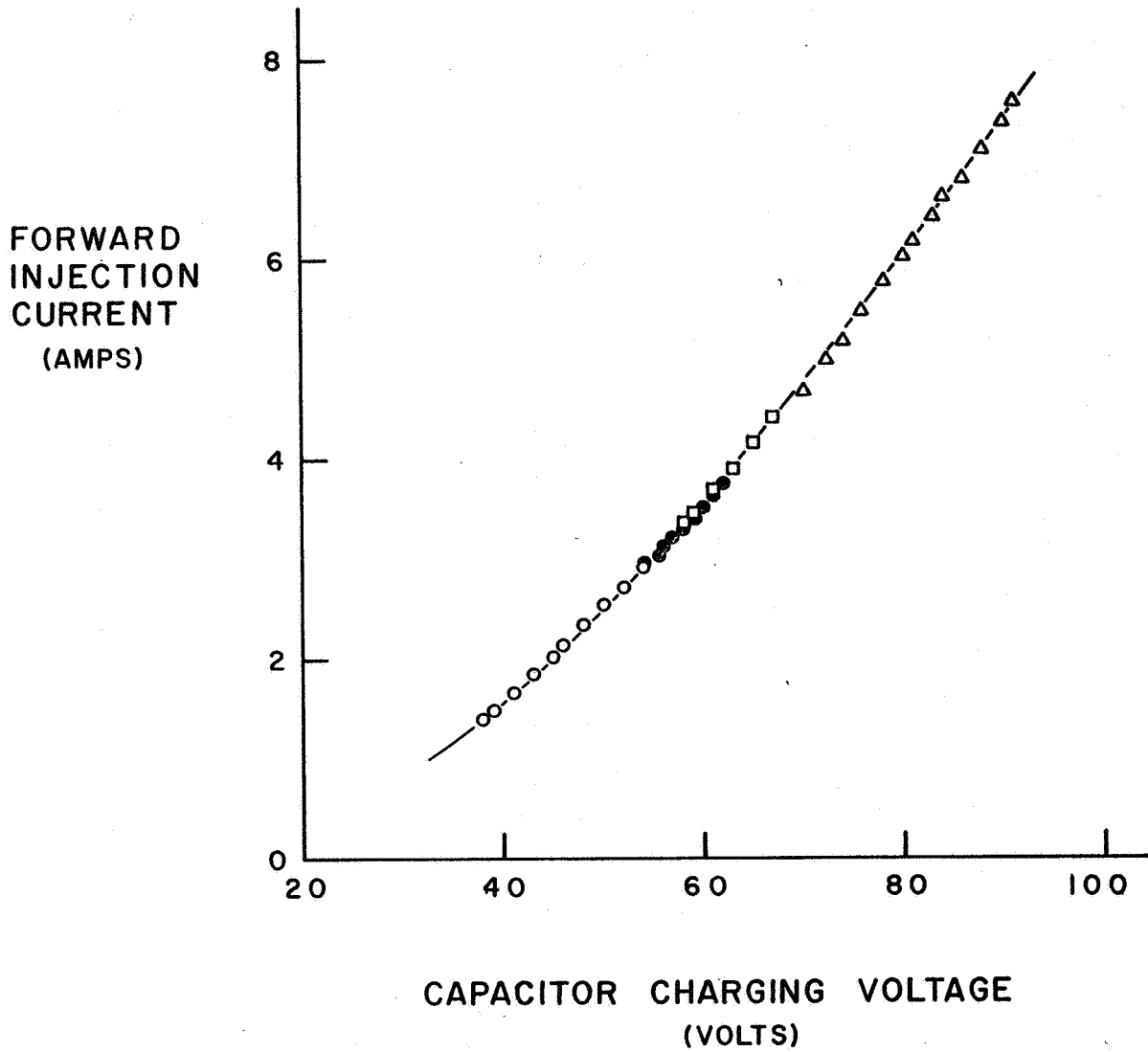
Fig. 6--High current forward I-V characteristics for GE H1D1 diode taken
at 77°K. The forward current is plotted against the capacitor
charging voltage.

● before this series of irradiations
□ after 1×10^{15} 1.2 MeV electrons/cm^2
O after electrical annealing
△ after 1×10^{16} 1.2 MeV electrons/cm^2

where

n_o = index of refraction,

ν = frequency

d = thickness of the active region,

$\Delta \nu$ = line width,

η = quantum efficiency,

ℓ = cavity length,

R = reflectivity of the ends of the cavity, and

α = loss in the system.

If the chief cause of the change in laser threshold upon irradiation is a decrease in EL efficiency, we may simplify this equation to

$$j_t = \frac{K}{\eta} \quad , \tag{2}$$

where K includes all the other terms, now assumed independent of radiation dose. If j_t^o is the threshold current density and η^o the EL efficiency before irradiation, and j_t^i and η^i the corresponding values in the ith state of radiation damage, then

$$j_t^i - j_t^o = \frac{K}{\eta^i} - \frac{K}{\eta^o} = \frac{K}{\eta^o}\left[\frac{\eta^o}{\eta^i} - 1\right] \quad . \tag{3}$$

Since K/η^o is independent of the state of irradiation, a plot of $j_t^i - j_t^o$ vs $(\eta^o/\eta^i) - 1$ should be a straight line through the origin.

(η^o/η^i) was measured at 77^oK after each of a number of irradiation and annealing steps. The laser threshold current was also measured after

15

each step. η^o/η^i was determined by measuring the non-coherent EL output from the diode as a function of current at currents below laser threshold. The EL output was substantially proportional to the injection current, decreased with successive irradiation steps and increased again upon annealing. Plots of EL output vs injection current are shown in Fig. 7 for a diode before irradiation (top curve) and for various stages of irradiation damage (lower curves). η is then taken to be proportional to the EL output at some arbitrary current, in this case 1 amp, and the ratio η^o/η^i is determined at this current.

Figure 8 shows a plot of $j_t^i - j_t^o$ where j_t is the threshold current in amps (proportional to j_t) vs the values of $(\eta^o/\eta^i)-1$ measured in this way. The points lie near a straight line drawn through the origin. There are small systematic deviations at high threshold currents, presumably indicating that other mechanisms of damage are becoming important after a large dose of radiation. However, the results indicate that the chief cause of the change in laser threshold after irradiation is a decrease in EL efficiency.

The decrease in EL efficiency with dose is not linear, or exponential, as shown in Fig. 9 for the case of electron irradiation. A simple model for radiation damage is one in which centers are introduced in a concentration proportional to radiation dose and serve as sites where non-radiative recombination can occur. These centers then compete with radiative centers for the recombination of minority carriers injected as forward current. The EL efficiency may then be expressed as

$$\frac{\text{total lifetime}}{\text{radiative lifetime}} = \frac{1}{A + B\varphi} \quad ,$$

where A and B are constants and φ is the fluence of high energy particles.

We may write

$$\frac{\eta^i}{\eta^o} = \frac{1}{A + B\varphi} \quad .$$

Since $\eta^i = \eta^o$ when $\varphi = 0$, $A = 1$ so that

$$\left[\frac{\eta^o}{\eta^i} - 1 \right] = B\varphi \tag{4}$$
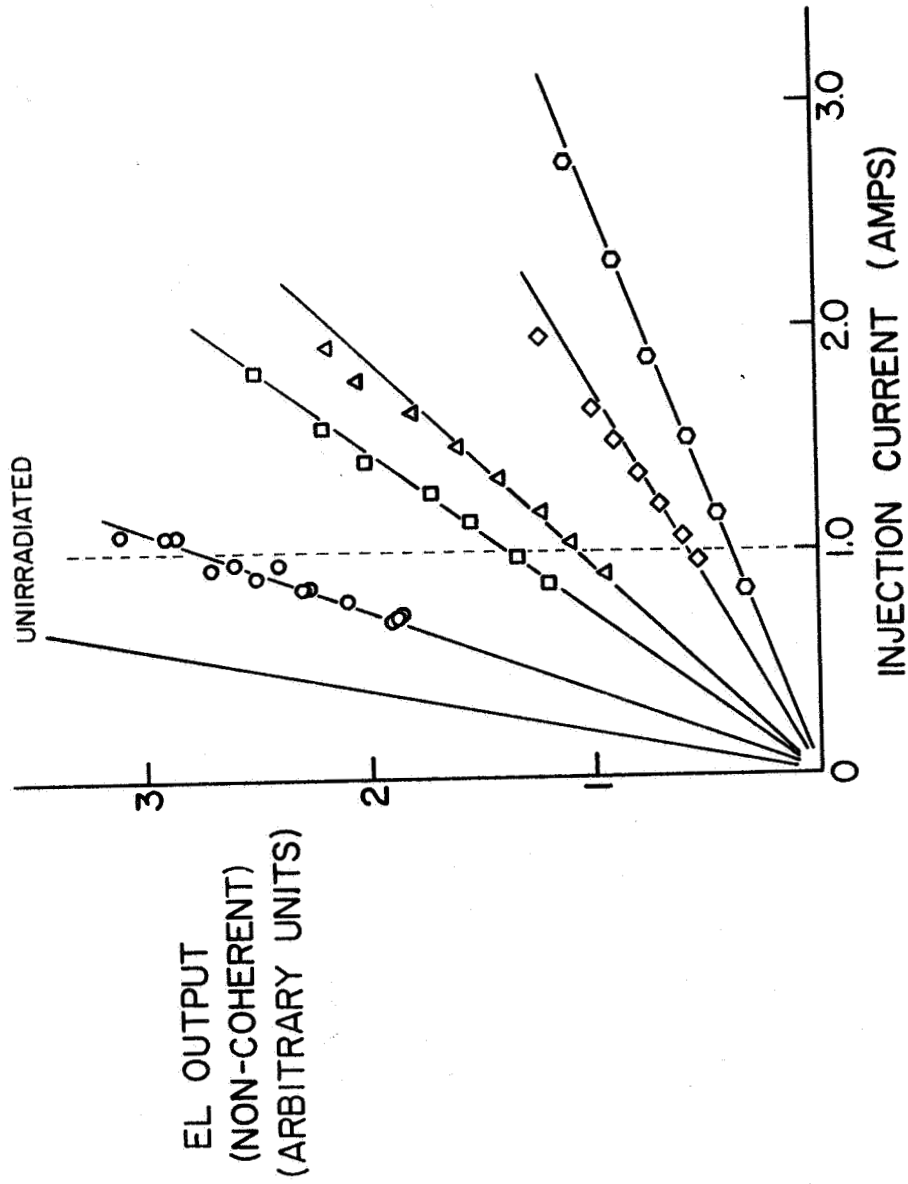
Fig. 7--Electroluminescent (non-coherent) output from GE H1D1 diode at 77°K as a function of forward current (below threshold) at several stages of irradiation. Lower lines represent successively increasing effects of irradiation.

17
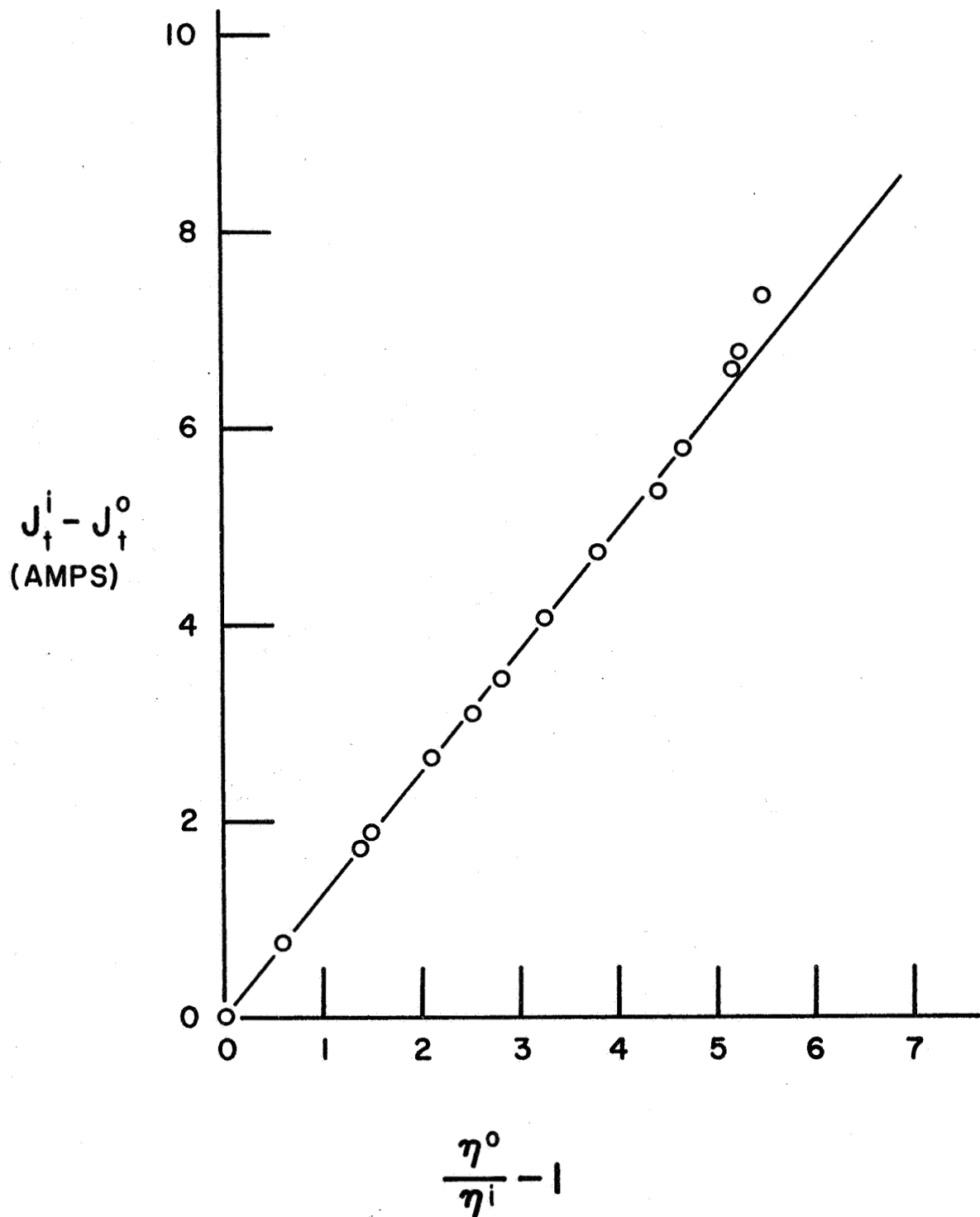
Fig. 8--$J_t^i - J_t^o$ (change in threshold current in amps) vs $(\eta^o/\eta^i) - 1$ (η is proportional to electroluminescent efficiency) for GE H1D1 diode at 77°K at various stages of irradiation. Original threshold current (J_t^o) was 1.5 amps.
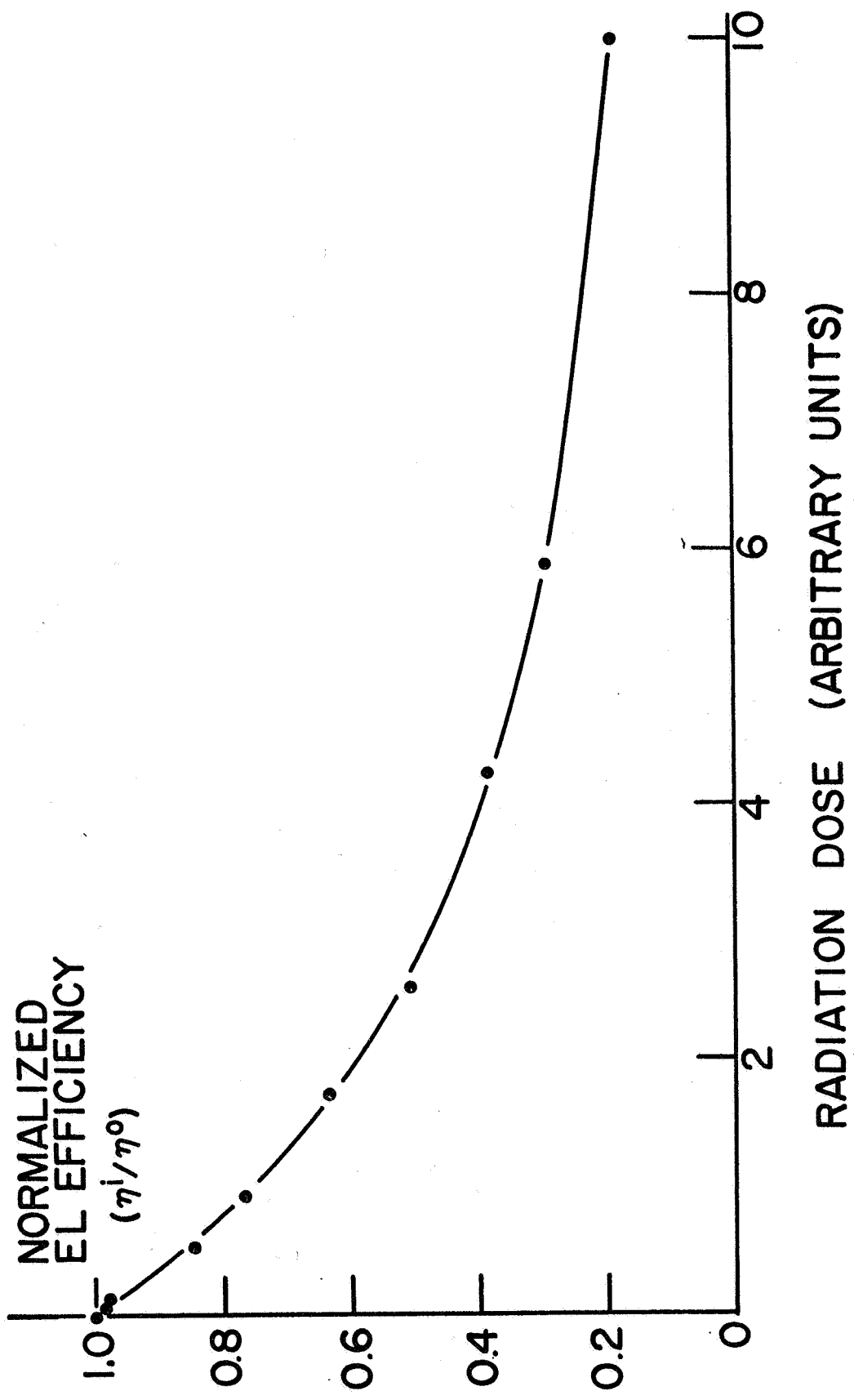
Fig. 9--Normalized electroluminescent efficiency (η^i/η^o) vs radiation dose, in arbitrary units

19

A plot of $(\eta^o/\eta^i) - 1$ vs φ should then be a straight line through the origin, as is shown to be the case in Fig. 10.

Values of B were determined for several diodes of different manufacture using 30 MeV electrons. The values obtained are shown in the following table:

Diode Type	GE H1D1	RCA TA2628
$B(electron^{-1}cm^2)$	3×10^{-13}	5×10^{-13}

It can be seen that the values are reasonably close.

The results cannot be directly compared with those of Aukerman and co-workers, since the present measurements are taken at much higher current densities, and are as a function of current rather than voltage. A detailed understanding requires a knowledge of the mechanisms of radiative recombination that are active in the diode under study. Work of this kind, on EL diodes and bulk GaAs is currently being performed under Contract AF 19-(638)-5838. The simple model is adequate at present.

Since the laser threshold current is proportional to $(\eta^o/\eta^i) - 1$, and this quantity is in turn proportional to radiation dose, the change in laser threshold current upon irradiation is also expected to be proportional to radiation dose. This is, in fact, found to be true. An example is given in Fig. 11 for an RCA TA 2628 diode irradiated with 30 MeV electrons. Once again, there is a deviation at high doses.

The change in laser threshold current can then also be used as a measure of the relative effectiveness of different irradiations, e.g. of different types or energies of charged particles.

2.4   Effect of Electron Energy, Comparison Between Effects of Electrons, Protons and γ-Rays

Figure 12 shows a typical result for a series of irradiations with electrons with nominal energy in the range 0.5 to 1.3 MeV. Each irradiation was of the same fluence, 1×10^{15} electrons/cm^2. While irradiation with 0.6 and 0.7 MeV electrons gave negligible damage, the shift in

Fig. 10--$(\eta^o/\eta^i) - 1$ vs radiation dose, in arbitrary units

RADIATION DOSE (ARBITRARY UNITS)

$\frac{\eta^o}{\eta^i} - 1$
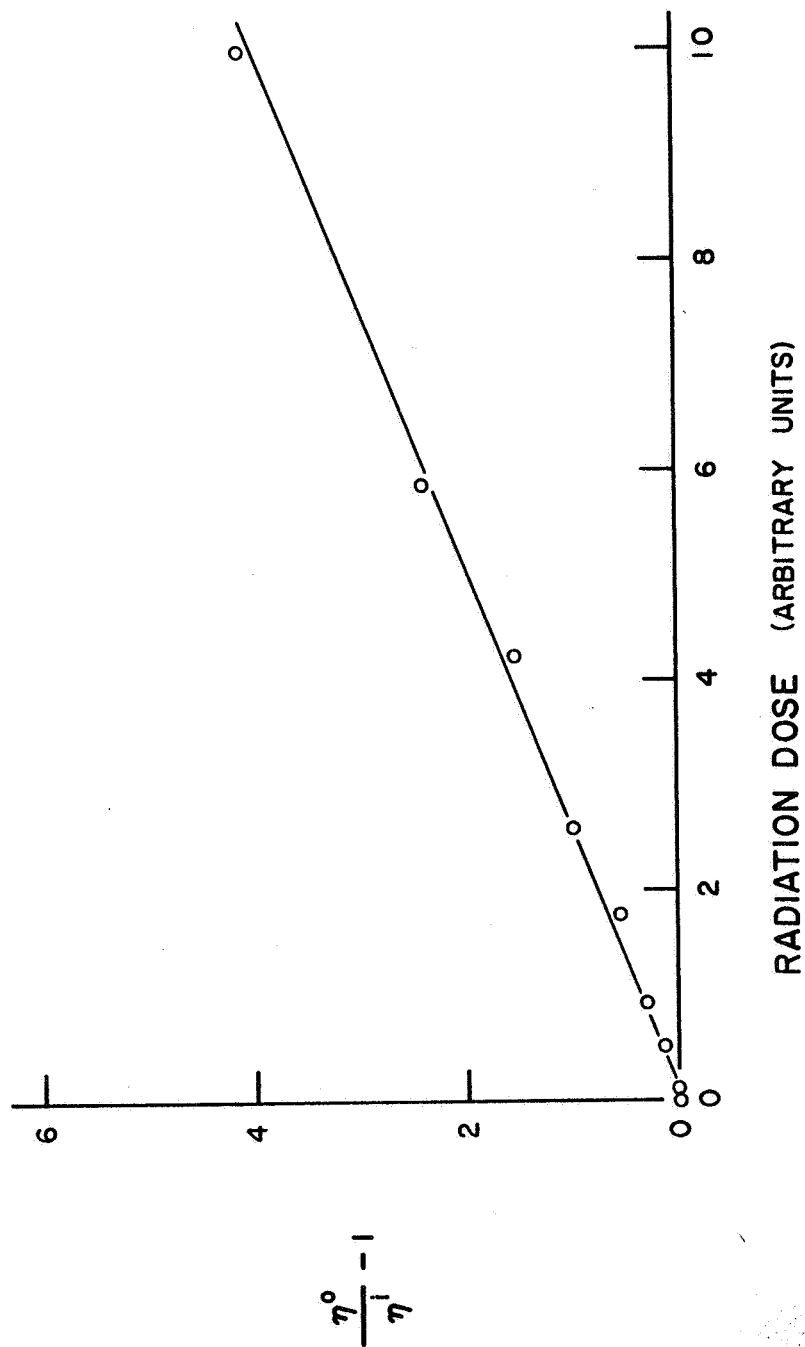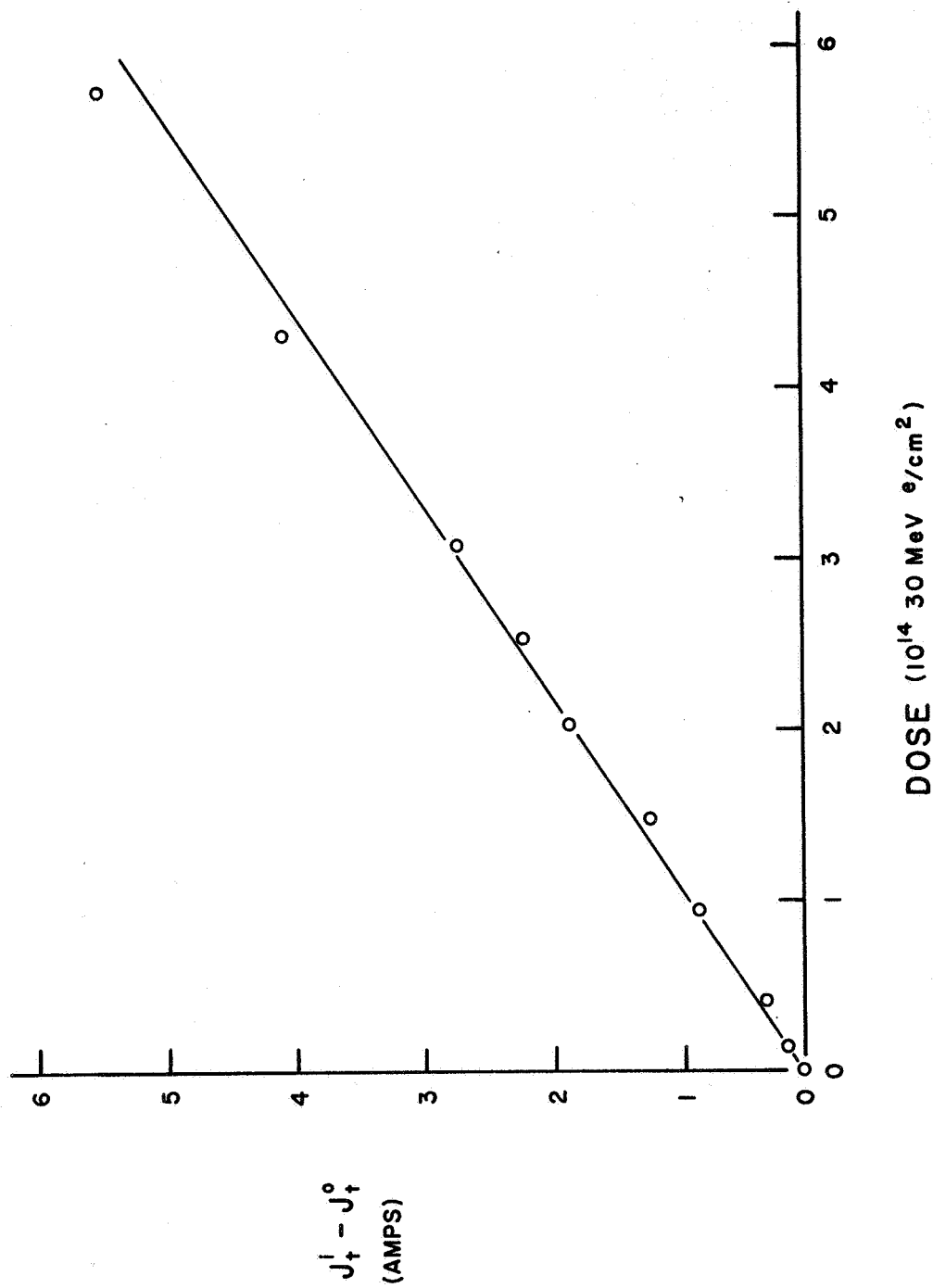
Fig. 11--$J_t^i - J_t^o$ (change in threshold current in amps) for RCA TA 2628 diode measured at 77°K, vs fluence of 30 MeV electrons.
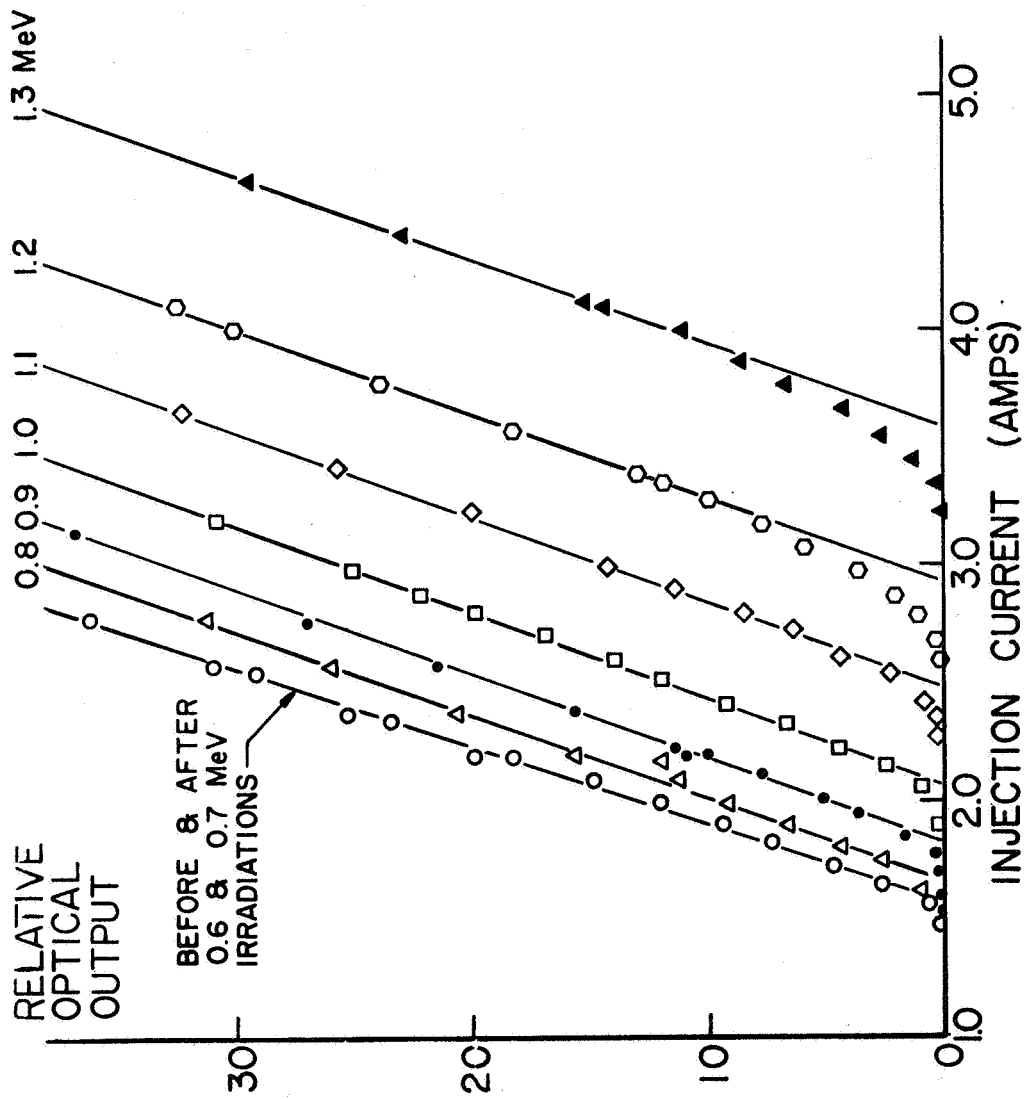
Fig. 12--Optical output vs injection current of GE H1D1 laser diode measured at 77°K after irradiation with 10^{15} electrons/cm^2 of machine energies indicated

threshold grows larger for each of the other energies as they are increased. The shift in threshold may be used to give a plot of relative damage (arbitrary units) vs electron energy. It is necessary to correct the nominal (machine) values of electron energy to the most probable energy of the electrons reaching the junction region of the diode. This correction is made necessary by the energy loss of the electrons in the exit window of the accelerator, in the diode top electrode, and in the GaAs itself.

The electron source used was the Convair Dynamitron accelerator. This machine is a cascade-rectifier type of accelerator and will deliver up to 1 ma direct current with energies up to 2.8 MeV. The machine is calibrated against known radioactive standards, and its beam energy is read by a voltmeter readable to 1% full scale. The current was measured by a Keithley model 610A electrometer with a 1% full-scale accuracy. For the GaAs diode irradiations, the current density was measured with a Faraday cup with a carefully machined entrance hole of known area, and was limited to a low enough value to avoid heating effects.

The accelerator window was 5×10^{-3} cm thick titanium and the cryostat window 1×10^{-3} cm thick Mylar. The GaAs itself had a junction depth of $\sim 7.6 \times 10^{-3}$ cm and the gallium-tin top contact had a thickness of $\sim 5 \times 10^{-3}$ cm.

The electron energy degradation in the system can be calculated by using an empirical electron range-energy relationship due to Glendenin:[20]

$$R = 0.407 \left[(E_i)^{1.38} - (E_t)^{1.38} \right] , \qquad (5)$$

where

$R = \rho t$, is the range of the particle in g/cm^2,

ρ = density of the material,

t = thickness of the material in cm,

E_i = incident electron energy in MeV, and

E_t = most probable energy of the particles at a depth t in the material.

This equation is valid for most materials and for energies in the region

$$0.15 \text{ MeV} < E < 0.8 \text{ MeV} \ .$$

Using this equation, and the properties of the windows and diode, we have estimated the most probable energy of the electrons in the region of the diode junction. This correction is partially compensated by another effect: since the electrons are scattered slightly as they lose energy they traverse a path longer than the penetration depth and thus have a higher probability of producing displacements;[21] this effect is, however, small and has been neglected. The correction is large for lower energies (e.g., for a machine energy of 0.5 MeV the calculated energy of the electrons at the junction is 0.27 MeV), but becomes less important at higher energies.

Correcting the energy scale in this way, a plot of relative damage vs electron energy can be made. Such a plot is shown in Fig. 13.

The plot has the form of a straight line with an intercept at just over 0.5 MeV, corresponding to an apparent threshold energy for radiation damage. This type of dependence on electron energy is that expected for a displacement radiation effect, where centers are formed by displacement of an atom from its site by the collision of an electron. The linear dependence of damage on electron energy above threshold is similar to that found in the careful work of Grimshaw and Banbury.[16] They obtain good agreement between displacement theory and their results if they take E_d, the energy necessary to displace an atom, as 17-18 eV, corresponding to a threshold electron energy, on the sharp threshold model, of 0.4 MeV.

The displacement threshold that we find is somewhat higher than that of Grimshaw and Banbury,[16] who used carrier removal as a criterion, and very much above that reported by Bauerlein,[15] who used the deterioration of a photovoltaic response as a criterion and found displacement thresholds at electron energies of 230 and 275 KeV, which he attributed to separate displacement thresholds for Ga and As. Loferski and Wu[17] reported a threshold between 275 and 288 KeV. Arnold[22] finds an optical emission appearing after exposure to electrons of energy greater than 1 MeV and suggests that this corresponds to time displacements, and that the effects at lower electron energies may be associated with the breakup of grown-in defects (interstitial vacancy pairs) thought[22] to be present in as-grown GaAs.
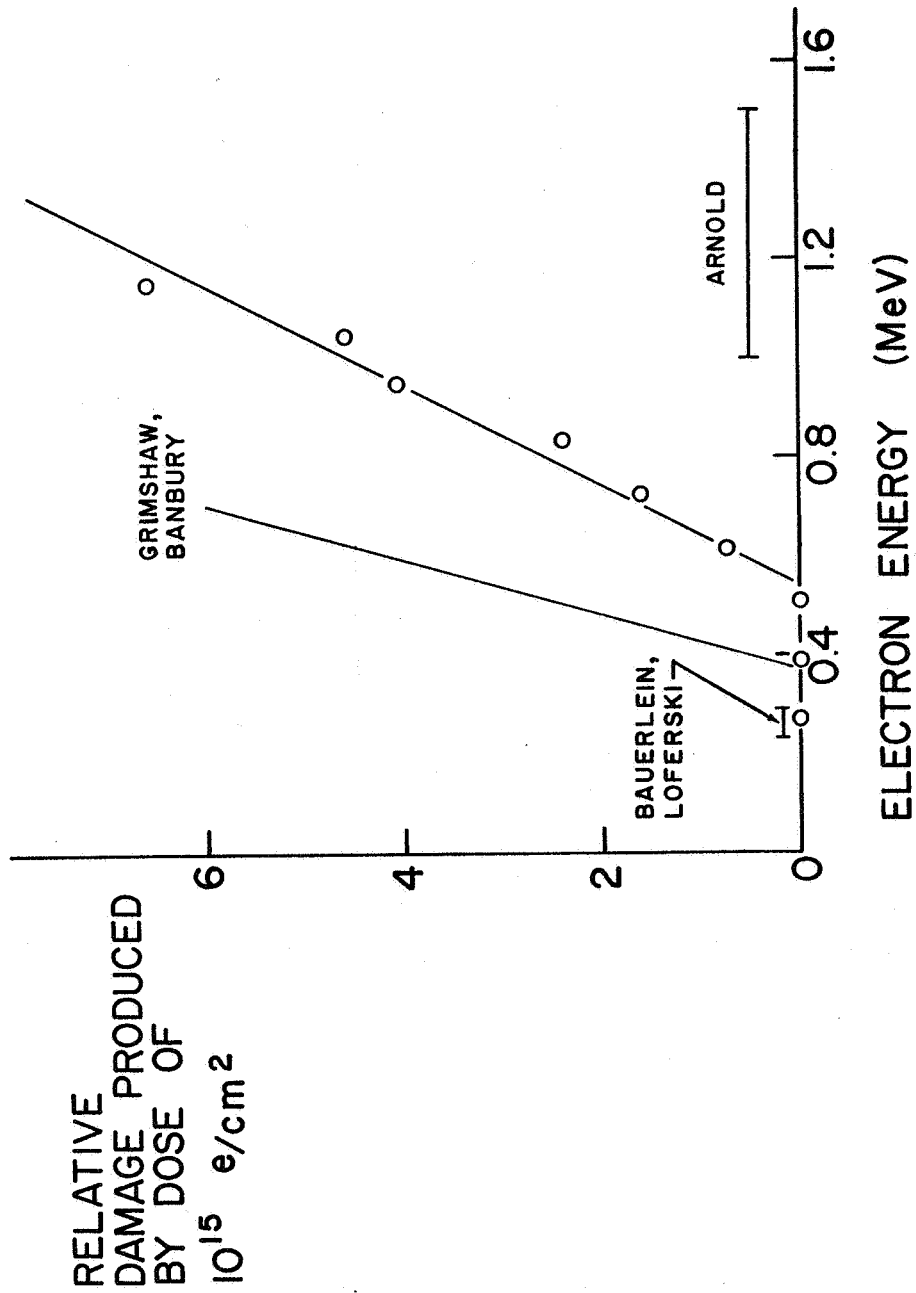
Fig. 13 -- Relative damage effects of constant doses of 10^{15} electrons/cm^2 vs electron energy at junction (see text). Also shown are the threshold values given by Bauerlein,[15] Loferski and Wu[17], and Arnold[22], and the relative damage vs energy curve given by Grimshaw and Banbury[16] (the slope of this line is arbitrary).

Exposure to γ-rays in a shut-down TRIGA reactor (residual γ-rays from radioactive fission products left after the reactor has been operating) produced no change in laser output, even after doses in excess of 1 megarad. This indicates clearly that no ionization-type effects are active in producing damage in GaAs lasers. The γ-rays produce Compton electrons in the GaAs, which could produce displacement radiation effects if their energy and their equivalent flux were high enough. The fission product γ-rays used have a typical energy of ~ 0.7 MeV, and this corresponds to a mean Compton electron energy of ~ 0.3 MeV, so that most of the Compton electrons produced are ineffective in producing displacements.

The effects of 32 MeV protons from the University of Southern California proton linac, and of 30 MeV electrons, from the General Atomic Electron Linear Accelerator, have also been studied. These facilities were described in the previous report.[1]

For the 30 MeV electrons, dosimetry was performed using a thin calorimeter replacing the sample. The thin calorimeter was either a thin copper foil with a thermocouple attached to it, or a thermistor. In either case, the temperature rise produced by a single pulse of electrons was measured, using a microvoltmeter and recorder to measure the output of the thermocouple in the first case, and the off-balance voltage of a Wheatstone bridge in the second case. The temperature rise gives the energy deposition in the calorimeter, which can readily be related to the electron flux for high-energy (> 1 MeV) electrons. The diode was then irradiated with a succession of similar pulses, the repetition rate being kept low enough to avoid heating effects, and the number of pulses was recorded on a scaler. The constancy of dose from pulse to pulse was measured using a current-transformer ring monitor on the output of the electron beam tube. The output of the monitor is fed to an oscilloscope, and adjustments are made to the accelerator as needed to keep the current constant from pulse to pulse.

Proton dosimetry was performed as follows. An argon ionization chamber was placed at the exit window of the accelerator and used to monitor the proton output flux. After passing through the monitor, which causes some scattering, the beam passed through a 50 cm vacuum drift tube and was collimated by a 1 cm^2 aperture machined in an aluminum-lead stopping block. The beam current passing through the aperture was then measured by a Faraday cup and used to calibrate the argon ionization chamber to give the effective proton flux at the sample position. The signal from the ionization chamber was then used as a beam monitor by the accelerator operator and was also integrated to give the fluence (accumulated dose) for each irradiation. The uniformity and size of the proton beam at the sample position was checked by the coloration of a glass plate. The plate showed uniform coloration over the 1 cm^2 area.

27

The protons experience a significant energy loss in passing through the argon ion chamber, windows, and air. On the basis of previous experiments, the accelerator staff estimate this energy loss as 1.9 MeV. A further loss, estimated as 0.1 MeV, occurs as the protons penetrate to the junction region of the GaAs laser diode. For a machine energy of 32 MeV, the effective energy of the protons is estimated to be 30 ± 0.5 MeV.

The results of proton irradiation on GaAs diodes were found to be generally similar to those of electron irradiation, i.e., a change in laser threshold current and a decrease in electroluminescent output. Figure 14 shows the change in the curves of laser output vs injection current produced by successive proton irradiations. As in the case of electron irradiation, the main change is a shift in threshold current, with little change in the slope of output light vs input current. Figure 15 shows the corresponding effects on electroluminescent (non-coherent) output. Figure 16 shows the change in threshold current plotted vs proton dose for the diode of the previous two figures and for another diode of the same type number. Threshold current is measured by extrapolating the plot of light output vs input current taken at high light output, to zero output. This extrapolation is done to avoid difficulty with the non-sharp thresholds after irradiation. Figure 17 shows corresponding plots of $[(\eta_o/\eta_i) - 1]$ vs dose. The differences between the two diodes of the same type represent the typical variation found. This variation is attributed to differences in construction details and doping level.

As described in the previous report under this contract, calculations have been made at General Atomic on the relative numbers of defects expected to be produced by electrons and protons of various energies. These calculations[22,24] have been made for Ge, and should be reasonably good for GaAs, since the cross sections for the various processes vary only slowly with atomic number (nuclear inelastic scattering is neglected). The predicted defect introduction rates, relative to 30 MeV electrons, are

1.5 MeV electrons	2.3 MeV electrons	30 MeV protons
0.18	0.27	20

while the experimental values found for germanium using several different criteria for damage, ranged from

0.06-0.18	0.18-0.36	13-41

For the results reported here on GaAs laser diodes, the corresponding
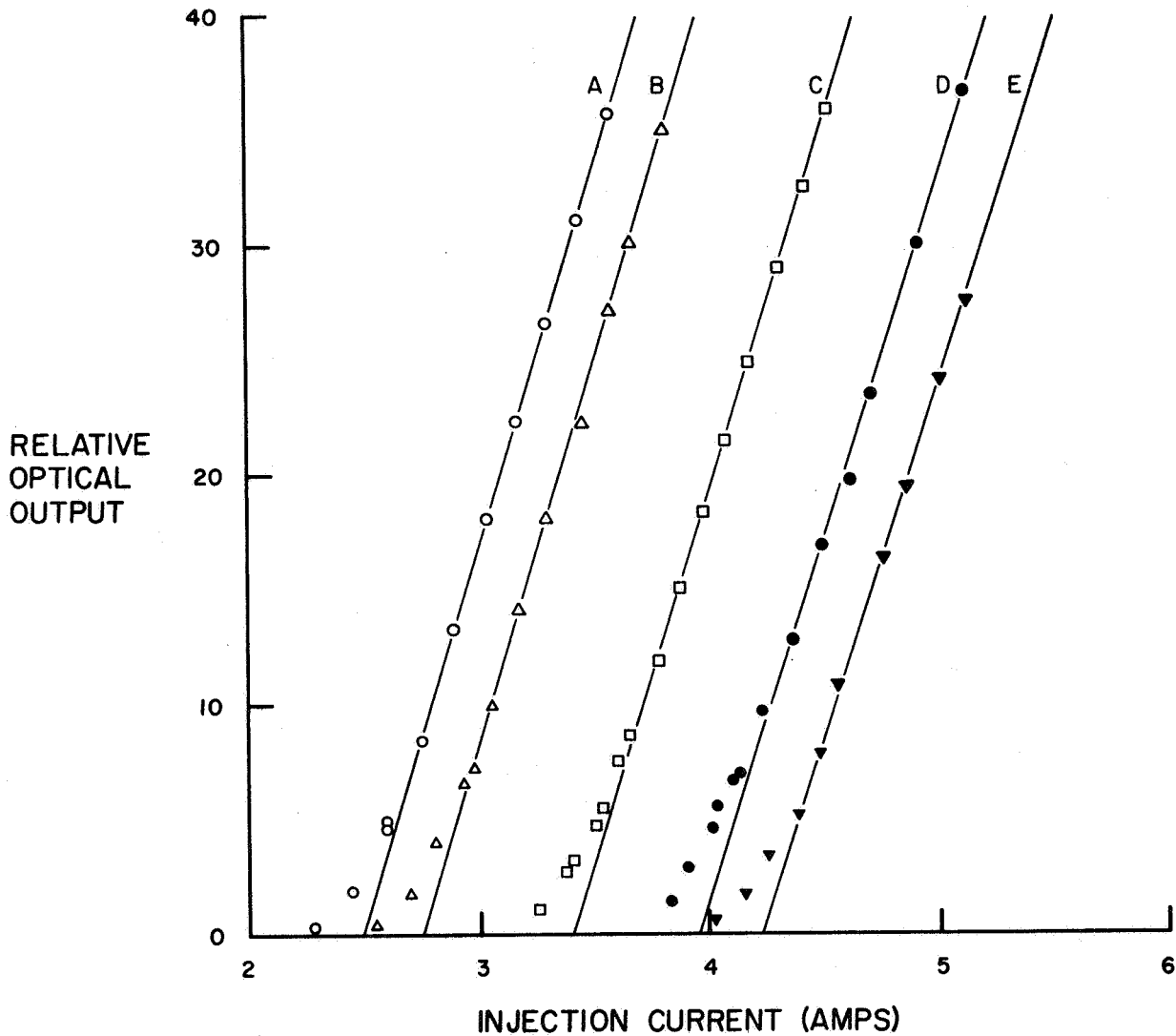
Fig. 14--Relative optical output (laser emission) as a function of forward
injection current for GE H1D1 laser diode No 4354 after
various stages of irradiation. Line A shows the before-
irradiation optical output, and succeeding lines show the
output after proton fluences of (B) 0.7×10^{12}, (c) 1.8×10^{12},
(D) 1.7×10^{12}, and (E) 0.9×10^{12}, respectively
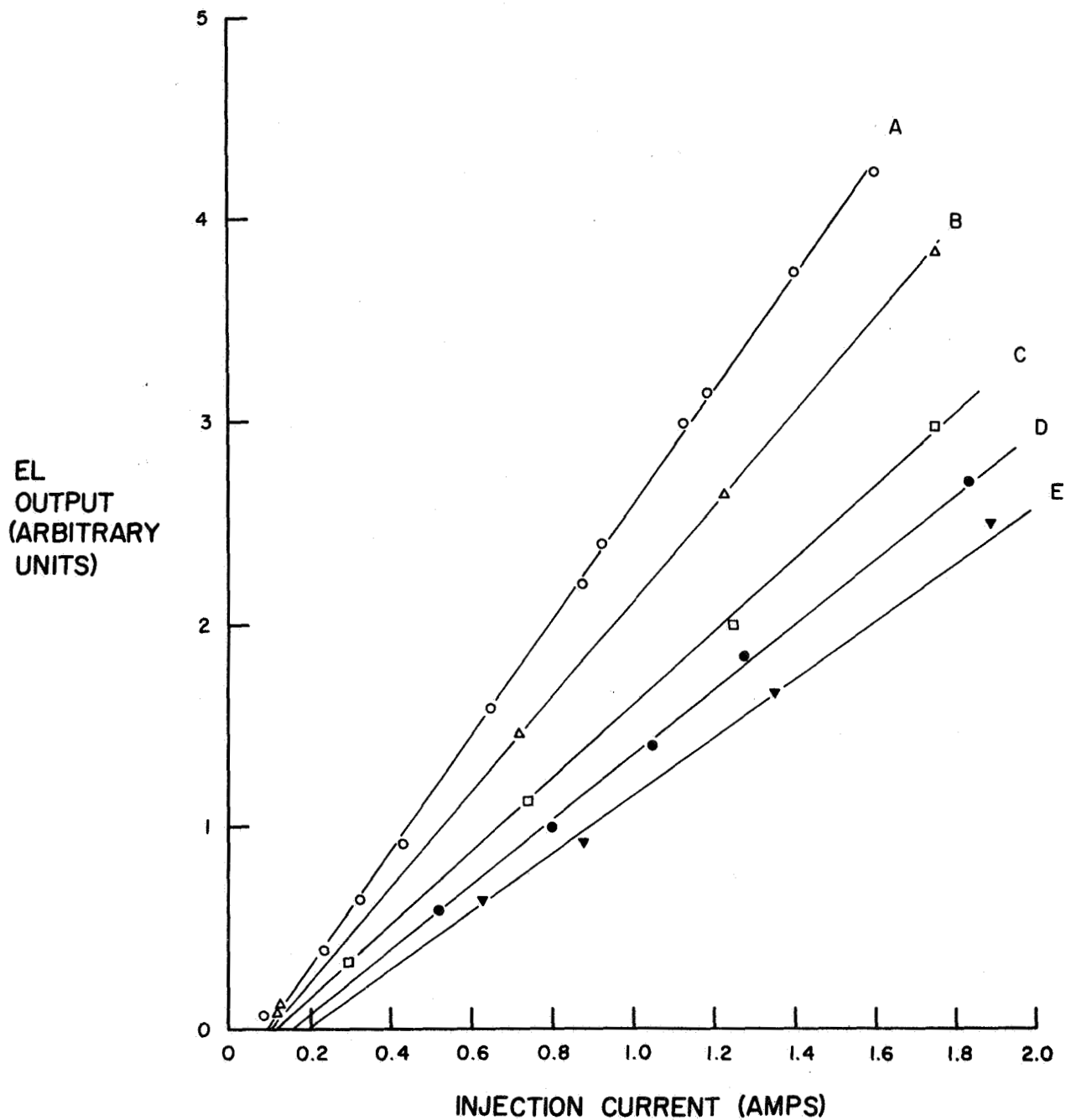
Fig. 15--Electroluminescent or non-coherent light emission from
GE H1D1, No. 4354, laser diode at 77°K as a function of
forward injection current at several stages of proton
irradiation.   Line A shows the before-irradiation output
of the laser; succeeding lines show the efficiency after
proton fluences of (B) 0.7×10^{12}, (C) 1.8×10^{12},
(D) 1.7×10^{12}, and (E) 0.9×10^{12}, respectively

30
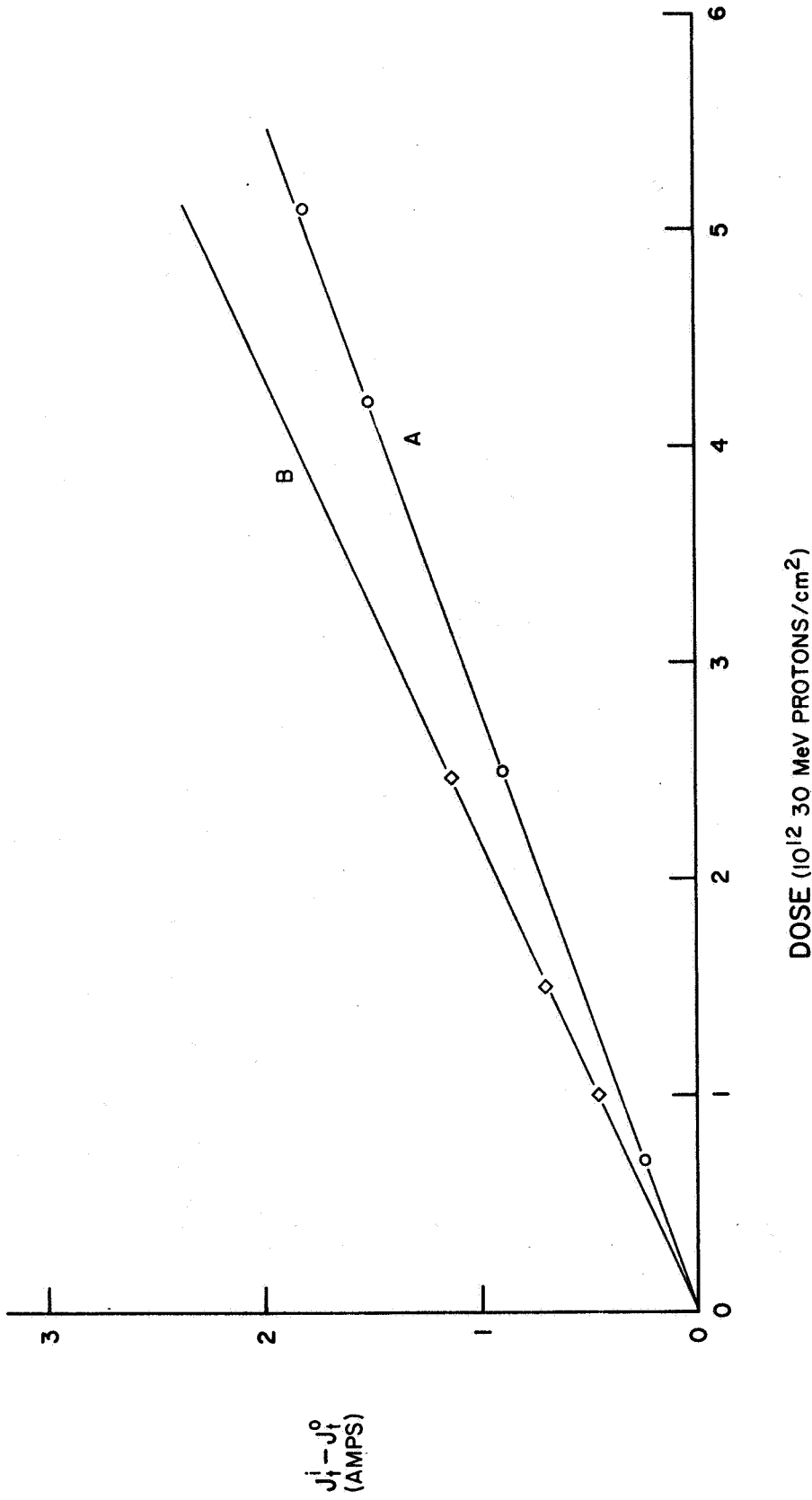
Fig. 16--The change in threshold current ($J_t^i - J_t^o$) vs proton fluence. (A) GE H1D1 No 4354, (B) GE H1D1 No 6393

31
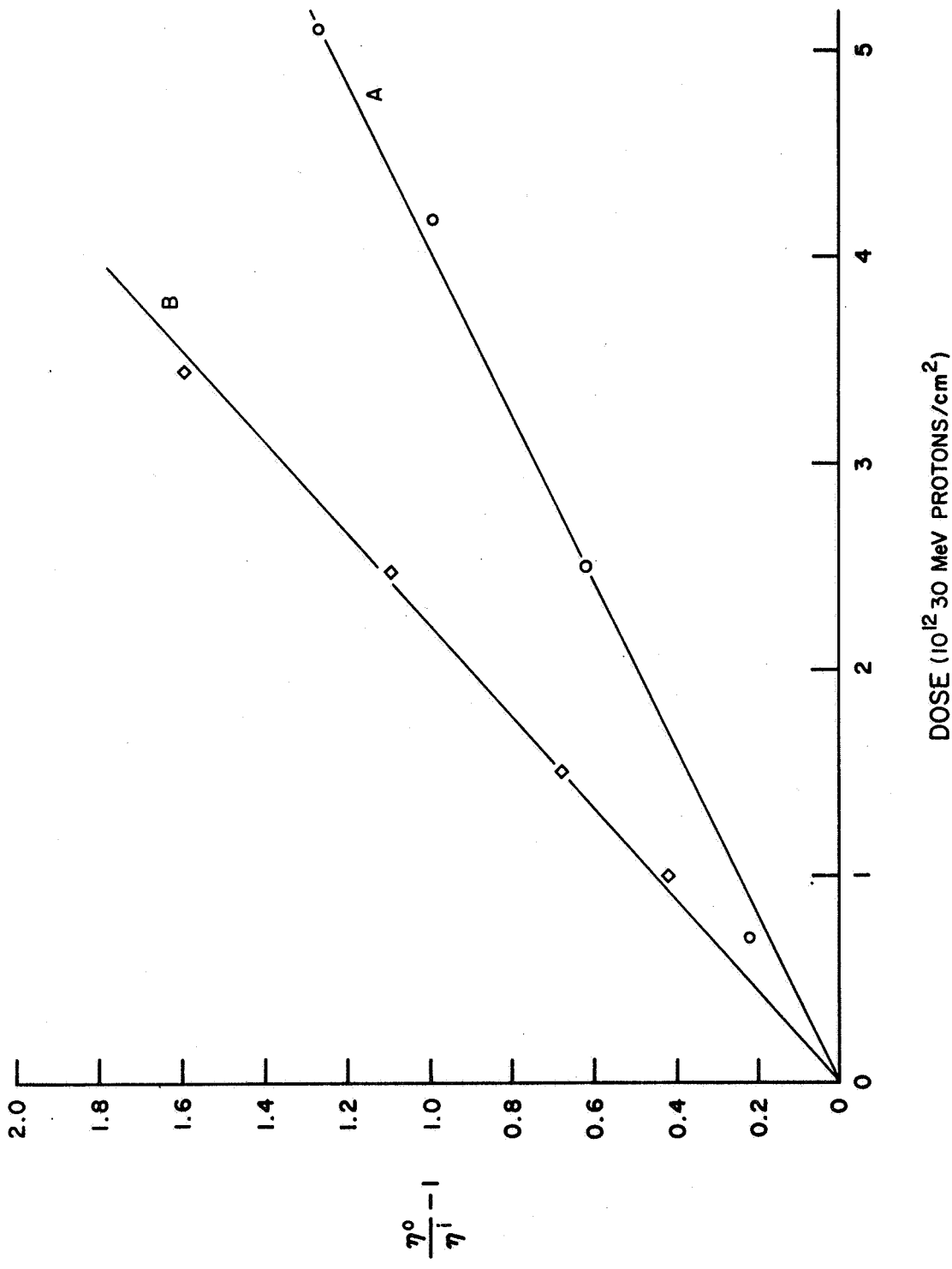
Fig. 17--The function $[(\eta_o/\eta_i) - 1]$ plotted vs proton fluence. (a) GE H1D1 No. 4354, (B) GE H1D1 No. 6393

figures are

0. 07-0. 08   -   22

These results were obtained by direct comparison, on the same diode, of
the effects of irradiation, with the different types and energies of radiation,
on the threshold current and spontaneous emission intensity. Care was
taken that only moderately small shifts in laser threshold were produced,
so as to keep in the linear region of threshold shift (see Fig. 11). As ex-
pected, measurements of threshold shift gave the same results as measure-
ments of decrease in EL output.

2.5   Effects of Temperature of Irradiation

Since GaAs diodes are commonly operated either at 77°K or at
300°K, it appeared worthwhile to compare the effects of irradiation at both
temperatures. The effects are found to be qualitatively similar, with a
small quantitative difference. The effectiveness of an irradiation at 77°K
is approximately 1.25 times that of the same irradiation at 300°K. An
example is shown in Fig. 18 of the shift in laser threshold, measured at
77°K, produced by two irradiations with 30 MeV electrons, at 77°K and
at 300°K. For each temperature, the shift in laser threshold at low doses
is found to be proportional to radiation dose, so that the effectiveness of
the irradiations may be compared by normalizing to constant dose. It
should be noted that warming a diode irradiated at 77°K to 300°K does not
remove any of the damage. This is discussed further in the next section.

2.6   Annealing

The annealing of radiation damage in GaAs has been studied. Simple
thermal annealing is not effective in most of the diodes that we have inves-
tigated because they have been limited to a maximum safe temperature of
$\sim 100^{\circ}$C by their method of construction. We have recently obtained some
diodes from Dr. N. N. Winogradoff of the National Bureau of Standards,
which should be annealable to $\sim 300^{\circ}$C, but as yet no measurements have
been made on these units.

Annealing at 100°C, even for extended periods, is not effective in
removing radiation damage. This can be seen in Fig. 19. where the line
at the right includes points taken at 77°K both before and after annealing
a radiation-damaged diode at 100°C for 15 minutes, by heating the heat
sink, to which it is mounted in the cryostat, to this temperature. No
recovery can be seen, and similar tests have shown no recovery after many
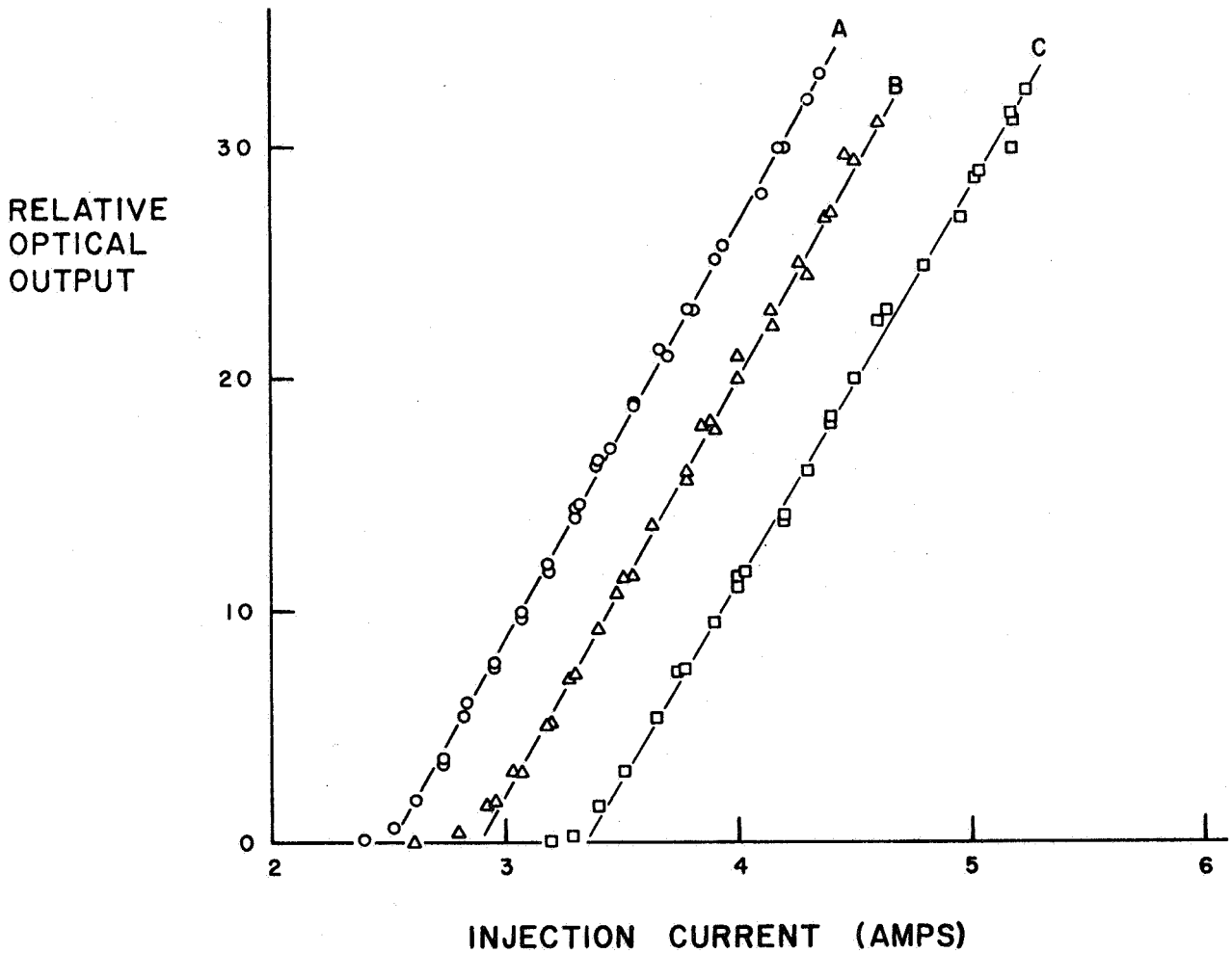
Fig. 18--Optical output of GE H1D1 diode measured at 77°K, vs injection current. Curve A, before, and B, after irradiation with 3.1×10^{13} 30 MeV electrons/cm^2 at 300°K; C, after a further irradiation with 2.7×10^{13} 30 MeV electrons/cm^2 at 77°K.
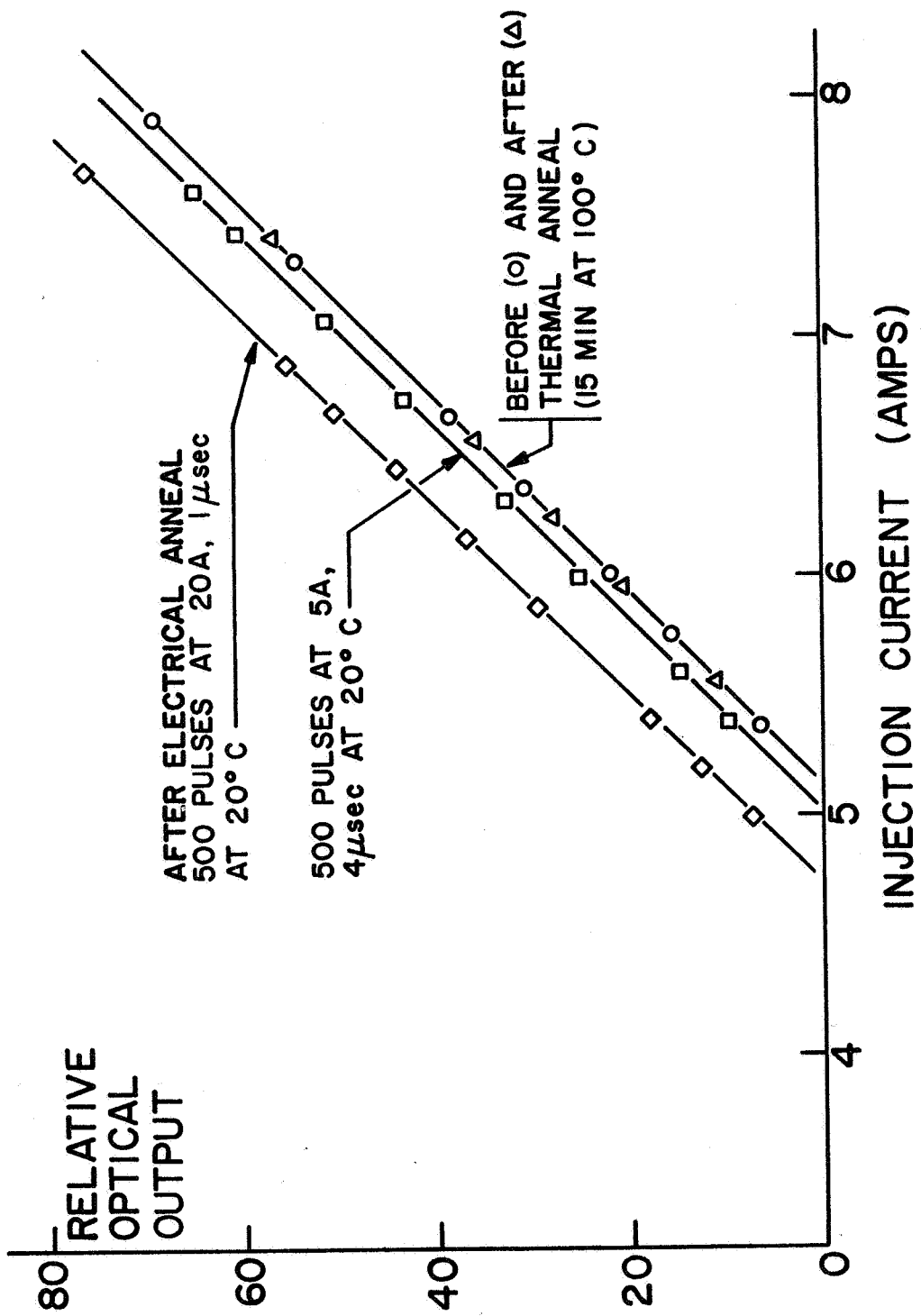
Fig. 19--Electrical and thermal annealing of radiation damage in GE H1D1 laser diode. Measurements of output made at 77°K.

hours annealing at 100°C. The initial threshold current of this unit was 1.5 amps. Aukerman and co-workers[12] report that annealing of radiation damage to GaAs EL diodes is slight at 150°C, and is reasonably rapid (an appreciable change being produced in 30 minutes) at temperatures above 250°C.

However, annealing of radiation damage can be produced by passing pulses of forward current through the diode. This process is illustrated in the two lines on the left of Fig. 19. Diodes can be nearly completely annealed by the passage of sufficient current pulses, although 10^4 - 10^5 pulses may be needed at room temperature. The efficiency of this annealing method increases with the magnitude of the current used, and the upper limit is set by damage to the laser diode. This damage occurs when the laser optical output power is high enough to damage physically the laser structure of the emitting faces.[23] Accordingly, as annealing proceeds, it is necessary to reduce the current used in order to keep the laser output power within safe limits.* Annealing by current pulses will occur without laser emission from the diode, so that laser emission, per se, is not necessary for the annealing process. The efficacy of annealing also increases with the temperature of the diode, being nearly zero at 77°K, and enhanced by a factor of ~ 5 at 100°C over that at room temperature. The extent of annealing is not affected by the time interval between pulses, and falls off approximately exponentially with the number of pulses so that after a large number of pulses the rate of further improvement is very slow. This behavior is shown in Fig. 20.

This annealing could be due to heating of the junction region by the current pulse, giving rise to thermal annealing of the radiation damage, without thermal damage to the rest of the diode structure. Alternatively, it could be due to some nonthermal effect of the current pulse. At present, the second explanation is thought to be correct. Annealing is produced by short pulses (1 μ sec or less). For substantial annealing to occur in this time, the temperature would have to be greatly in excess of 300°C. Simple calculations[25] of the increase ΔT of junction temperature give a value for ΔT of only a few degrees. This value is supported by measurements of the shift in output wavelength during the pulse. Even when 2 μ sec, 15-amp pulses are used at 77°K, the apparent optical line width of each mode, measured as indicated below, does not broaden by more than 3.0 Å from shift of the output wavelength of a mode during the pulse. Since this shift is ~ 0.5 Å/°C,[25] this corresponds to an increase in the temperature of the emitting region of only about 6°C during the pulse. An increase of temperature to room temperature during the pulse would produce a wavelength

---

*One diode was also destroyed from application of excessive voltage; an arc developed and burned away the diode at a current lower than laser threshold at room temperature after radiation damage.

36
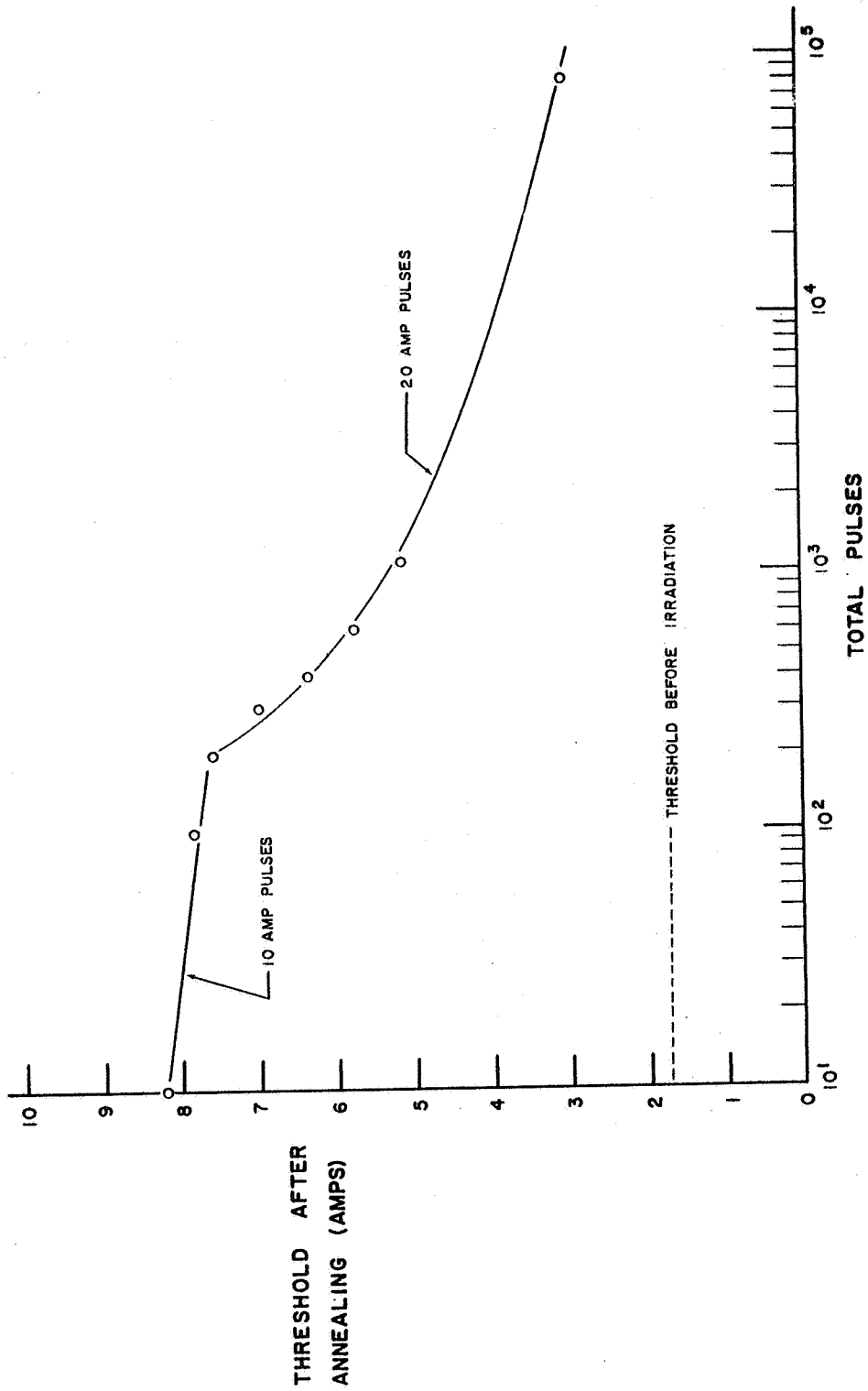
Fig. 20--Change of threshold by electrical annealing with 2 μsec pulses of forward current of peak amperage indicated. Threshold current in amps is plotted vs total number of pulses.

shift of ~ 600 Å. Application of such current pulses to the diode at 300°K will produce a somewhat higher ΔT, because of the lower external EL efficiency at 300°K, but the ΔT will still not approach the $300-500^\circ$C needed to explain the annealing.

The efficiency of annealing appears to be a function of the forward current, as shown in Fig. 19, where the effects of two pulse currents are compared. The pulses were adjusted to deliver the same energy,[25] but to differ in current, while both are kept short compared to the thermal time constant[25] of the whole diode. The high-current pulse is seen to be more effective. Application of the maximum safe reverse bias voltage for several hours does not produce any annealing of radiation damage.

The mechanism of this "electrical annealing" effect is not understood at present. However, it is very useful in producing recovery in irradiated diodes. The recovery is generally not complete, especially for heavy irradiations, but all the characteristics of the diode appear to return to those found for a smaller dose of irradiation, and the threshold becomes sharper as the threshold current decreases.

2.7   Effects on Output Wavelength and Near-Field Pattern

The output wavelength of GaAs laser diodes is also affected by irradiation. Most of our measurements were made by using a spectrographic technique, but a monochromator - photomultiplier combination was also used in some studies. The spectrographic method used a Jarrell Ash, Ebert-type 3.4 meter spectrograph with a 15,000 line-per-inch plane grating. The dispersion of this system is ~ 5 Å/mm in the first order. The laser diode in its cryostat was mounted on the accessory bar of the spectrograph. It is positioned by setting the spectrograph to the zeroth order and placing a linear source of light (a tungsten filament) at the film plane; this illuminates the slit. A lens system is used between the slit and the diode, and the diode is placed so that it is illuminated by the image of the slit, but is displaced towards the slit from the position of the focused image of the slit. This increases the size of the image of the diode on the slit. The emitting face of the diode is then aligned normal to the input axis of the spectrograph, by using a beam splitter to observe the light reflected from the emitting face. Final alignment is performed to maximize the signal received from the diode by a photodiode placed at the film plane.

The photographic plates used are Kodak 4 X 10 in. glass-based emulsions I-N and IV-N, developed by standard spectrographic techniques. The plates may be examined visually, or a Jarrell-Ash microdensitometer may be used to provide recorder traces of the film density. To provide

a wavelength reference, each plate is generally given argon reference lines by using an argon lamp in front of the spectrograph slit.

Typical rather poor spectra from a poorly performing Korad K-S1 laser diode operated at 77°K were shown before and after irradiation in Figs. 13 and 14 of Ref. 1. Spectra from a typical good-quality diode at 77°K are shown in Fig. 21. The two lines on the left, spanning all the spectra, are argon reference lines at 8408.21 Å and 8424.65 Å. The spectra are taken in groups. Each group of spectra contains spectra taken with different numbers of pulses to allow the film to record both the intense and the weaker modes without fogging. Spectra A,B, and C are of the broad-band, noncoherent light emitted when the laser is below threshold current; the slit width was 400 μ and the peak injection current 1.5 amp. Spectra D,E,F, and G are of emission just above threshold, with injection current 1.75 amp and slit width 20 μ Spectra H, I, and J are at a higher injection level, where signs of mode broadening are beginning to appear, some of the broadening being due to shift of mode emission wavelength with temperature during the current pulse, (2.25 amps, slit width 20 μ), although most of the broadening visible in the half tone is due to halation in the film. The mode pattern is symmetrical.

After irradiation, typical changes appear in the spectra. Figure 22 shows the spectra for the same diode as in Fig. 21 after exposure to a radiation dose of 1×10^{16} 1.2 MeV e/cm^2. Spectra A and B are of the spontaneous emission taken at 5.5 amps. When measured on the micro-densitometer these show no shift from the corresponding curves on Fig. 21. Spectra C,D,E, and F, taken at 6 amps, show a shift to the red. At slightly higher currents (6.6 amps), spectra G,H,I, and J are obtained. There are now two groups of modes, and each shows the effects of heating during the pulse. Similar splitting into two groups was found in the spectra from the Korad K-S1 diode shown in Figs. 13 and 14 of the previous report.[1]

Similar results are shown in the densitometer traces of Fig. 23. Trace A shows the mode structure of the emission of a GE H1D1 diode before irradiation, operated at 77°K in the pulsed mode at a forward current of 2 amps. Trace B shows the emission after irradiation at just above the new laser threshold (6 amps). The lines are now not regular, as is typical of poorer quality laser diodes, and have divided into two groups. Trace C shows the pattern at an input current of 6.6 amps chosen to give the same total intensity of optical output as for trace A. The splitting into two groups of modes is again plainly seen, but each mode is badly distorted by the temperature change produced by each pulse of input current. Since the EL efficiency has been lowered by the irradiation, a much larger fraction of the input energy is turned into heat in an irradiated diode than was the case before irradiation. At similar output powers, the mode structure

39

8408.21 Å 8424.65 Å
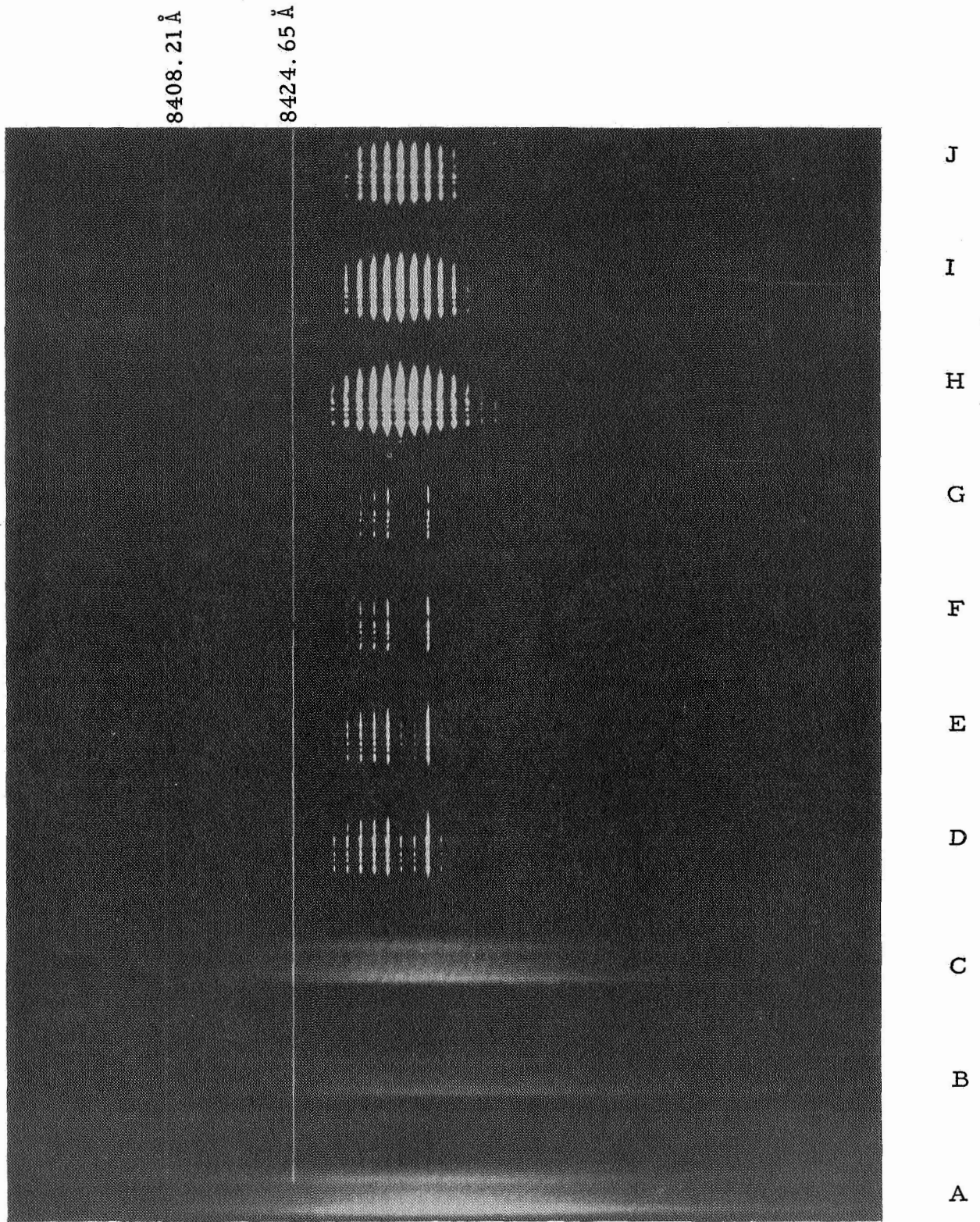
Fig. 21--Photographs of spectra from GE H1D1 diode operated at 77°K.
A, B, and C are of spontaneous emission, with peak injection
current 1.25 amp, slit width 400 μ; D. E. G and G are of stimu-
lated emission, current 1.5 amp, slit width 20 μ; H, I and J
are at 2.25 amps and a slit width of 20 μ.

40
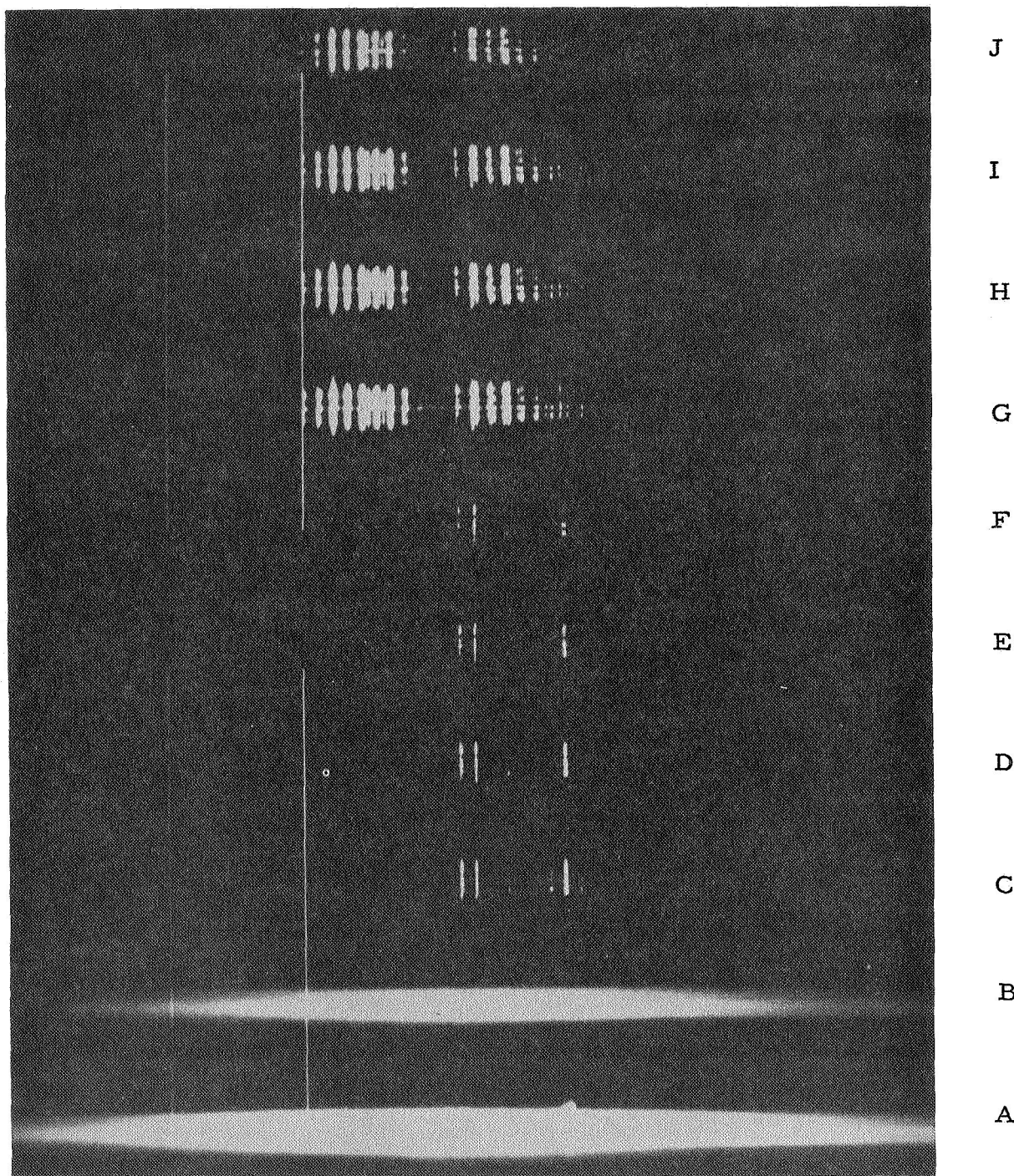
Fig. 22--Photographs of spectra from same diode as in Fig. 17, after irradiation with 1×10^{16} 1.2 MeV electrons/ cm^2. A and B, spontaneous emission, peak injection current 5.5 amps; C, D, E and F, stimulated emission at 6 amps; G, H, I and J, stimulated emission at 6.6 amps

Fig. 23--Densitometer recorder trace of spectrograph plate showing emission spectra of GE H1D1 diode operated at 77°K. A, before irradiation, at 2 amps; B, after irradiation at 6 amps; C at 6.6 amps

is then distorted, and this is associated with excess noise[26] and loss of coherence.

The shift in output wavelength and the splitting into two groups of lines are not yet understood. The width of each mode line, carefully determined with short pulses, does not increase upon irradiation. This width is a measure of the Q of the optical cavity,[27] and the absence of any increase indicates that irradiation does not introduce significant extra optical absorption loss in the GaAs laser diode. This is in agreement with the model used above; the chief effect of irradiation is to reduce the EL efficiency. The mode spacing is also found to be unaffected by irradiation, indicating that the index of refraction is not significantly changed by irradiation. Similar conclusions are reached by a study of the oscillations in the spectra of spontaneous emission, which we have measured in some laser diodes, and are due to multiple reflections of the spontaneous emission between the ends of the Fabry-Perot cavity.[28]

The spatial distribution of the laser emission along the junction is uneven.[25] This can be seen by examining the vertical distribution of intensity in the spectra of Figs. 21 and 22. The intensity profile represents that along the junction length, because of the focusing properties of the optical system used. The same effect can be seen in the photographs of near-field patterns shown in Fig. 24. A shows the uniform luminosity along the junction when an exciting current pulse below the threshold value is used to produce non-coherent emission. B shows a similar photograph of a single pulse above threshold, with a neutral density filter interposed which effectively avoids any record of the relatively weaker non-coherent light. The inhomogeneity of emission can be seen. At higher currents, more regions show laser action.

2.8   Conclusions and Recommendations

1.   The chief effect of radiation on GaAs laser diodes is to increase the threshold current.

2.   The change in threshold current at 77°K is typically an increase from 1 amp to 1.5 amp for a dose of 10^{15} 1.2 MeV electrons/cm^2.

3.   The effect is of the displacement type and needs a threshold energy of 0.55 MeV for electrons. The relative effectiveness has been measured for higher-energy electrons and for 30 MeV protons. Agreement with theory is reasonably good. Low energy γ-rays are ineffective.

43
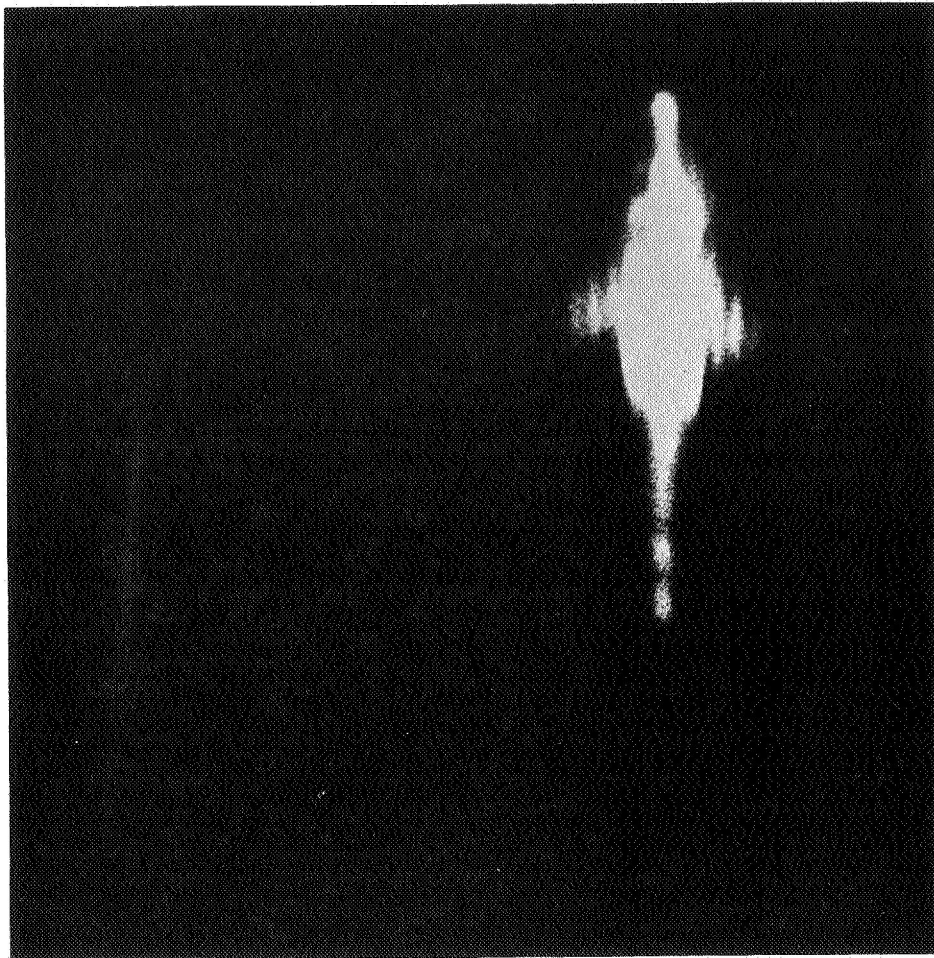
A   B

Fig. 24--Photographs of near-field patterns of emission from GE H1D1
diode operated at 77°K. A, below threshold, B above threshold

4. The effect cannot be annealed by heating to 100°C, but a procedure is described by which current pulses at 20°C can be used to remove most of the damage. Current pulses at 77°K are ineffective.

5. The mechanism of the effect is via a reduction in electroluminescent efficiency. A simple theory explains the increase of the damage with increasing dose, and typical curves are given.

6. From the results given it is possible to estimate the effects of a given radiation exposure on a GaAs laser diode. A damage constant has been measured for several types of laser diode relating the reduction in EL efficiency to the flux of 30 MeV electrons. The relative effectiveness of other energies of electrons and of 30 MeV protons has been measured and also given by theory. An estimated value for $(\eta^{o} / \eta^{i}) - 1$ can be obtained in this way. Equation 2 can then be used to relate the threshold current after irradiation j_{t}^{i} to that before irradiation j_{t}^{o}, since $j_{t}^{i}/j_{t}^{o} = \eta^{o}/\eta^{i}$.

7. The optical output spectrum is found to shift and break up into two groups of modes. There is also a greatly enhanced effect of heating during the pulse, if a diode is driven to give the same output power after irradiation as before. This affects noise and coherence.

8. The I-V characteristics at low forward voltages and currents may be changed by irradiation, while at the high currents needed for laser action there is no significant change.

9. Further work should be performed on CW lasers, on room temperature operating characteristics, and on other effects, such as time delays between the current pulse and the light emission pulse.[29] These need epitaxial diodes, which have recently been obtained. Further analytical work to develop a model for the output of a diode laser above threshold after radiation damage, would also be desirable.

III

OPTICALLY PUMPED LASERS

3.1   Previous Results

In the previous report[1] on this contract, a number of results on
the effects of radiation on optically pumped lasers were given. Nd-doped
lasers, in hosts of $CaWO_4$, glass, and YAG (yttrium aluminum
garnet), were studied, using flash lamp pumping. External dielectric
mirrors (i.e., detached from the rods) were used to form the optical
cavity. It was found that the pump energy needed to reach threshold is
increased by irradiation, while the slope of the plot of output power vs
input power is decreased. The effect was shown to be due to an additional
optical loss produced by the irradiation, and not to such phenomena as
broadening of the optical emission; changing line width; decrease in the
spontaneous emission lifetime; decrease in the reflectivity of the mirrors
forming the optical cavity; loss of pumping light by non-useful absorption
in the laser rod; effects on the transparency of the pumping flashlamp or
the light gathering efficiency of the laser enclosure; perturbation of the
level scheme; or sensitized energy transfer from the excited laser state
to color centers produced by the irradiation. This was demonstrated by
the use of an optical cavity capable of containing two laser rods in series,
as shown in Fig. 25. Only one rod is pumped, but either can be irradiated.
The same reduction in output is obtained when either rod is irradiated.
This shows directly that the effects of irradiation are due to optical loss.
A simple theory was developed, which predicted that if the photon lifetime
(which takes into account optical losses in the cavity and those due to re-
flectors) has the value t_o before irradiation, and another term, t_I, is
added to account for the additional optical loss due to irradiation, then the
pump power needed to reach threshold is increased by a factor of $(1 + t_o/t_I)$
over the pre-irradiation value, while the slope of the plot of output power
vs input power will be decreased by the same ratio. Such data as there
was, tended to agree with this prediction, but results were insufficient to
give a satisfactory confirmation of the theory. A brief discussion was given
of optical bleaching of the effects of irradiation, of thermal annealing, and
of spontaneous annealing at room temperature, all of which give rise to
dose-rate effects. Some results were given of a comparison of different
types of radiation, and of the relative susceptibilities of the different laser
materials.

Fig. 25--Two-rod optical cavity

RESONANT OPTICAL CAVITY

ANTI-REFLECTION COATINGS

TO OPTICAL SYSTEM

98% REFLECTING MIRROR

CRYSTAL UNDER STUDY

HOUSING WITH HELICAL FLASH LAMP WITH CaWO$_4$:Nd LASER ROD

100% REFLECTING MIRROR

¼ IN. LEAD COLLIMATOR WITH 1 IN. HOLE

ALUMINUM ATTENUATOR IF NECESSARY

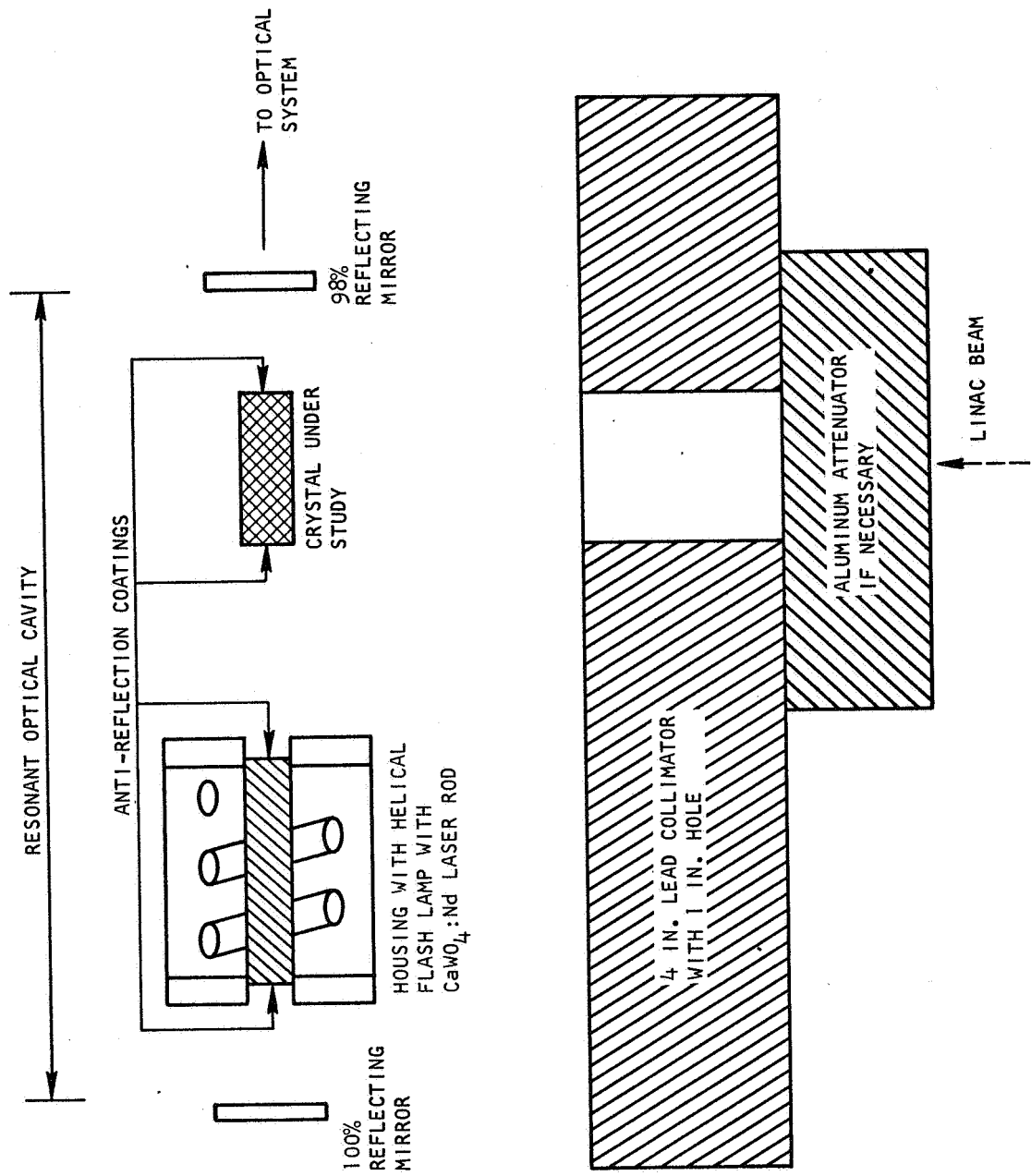LINAC BEAM

3.2   Materials and Mirror Arrangements

In the present reporting period, more measurements have been made on optically pumped lasers. The materials studied have again been Nd in $CaWO_4$, glass and YAG, and a small amount of work has been done with ruby. All of the laser rods except the glass were obtained from the Linde Company. The glass, type AO Lux 3835, was supplied by American Optical. The standard size of rod used was 3 mm o.d., by 30 or 50 mm long, although for comparison purposes several larger rods, up to 3/8 in. o.d., by 4 in. long in the case of $CaWO_4$:Nd, were also used. The ends were polished to 1/10 wave flatness and parallel to 10 seconds. Unless otherwise stated, the rods were used with dielectric mirrors evaporated directly on the ends of the rods, the reflectivities being 99% and 95%.

Some rods were left without dielectric mirrors and had anti-reflection coatings evaporated on their ends; they were then used in the optical cavity with external mirrors (Fig. 25). There was a surprisingly small difference in the threshold power and output-input curves obtained for similar (or identical) rods with the two different mirror arrangements, but it was simpler to make reproducible measurements on the rods with mirrors applied directly, since these did not have to be carefully aligned in an optical cavity.

The general type of results obtained are shown in Fig. 26. Reasonably straight lines are obtained for plots of laser output vs pump power. Ruby differs from the other three types of material examined; e.g., it has a higher output, under certain conditions (after irradiation) and is discussed first.

3.3   Ruby

Ruby becomes a striking orange color after irradiation; this serves as a convenient visual indicator of the state of its modification by radiation. However, this color, and the associated effects on the laser properties, are readily removed by optical bleaching. This severely complicates measurements, but, of course, indicates that the effects of radiation are not likely to cause operating problems in systems where the laser is pumped at reasonably frequent intervals.

Typical effects of irradiation are shown in Fig. 27. Line A in this figure represents the output-input curve before irradiation. After irradiation with 2.7×10^6 rads (fission product gamma rays) at 300°K, the rod was bright orange. The flashlamp was then fired at an output energy of 425 joules.
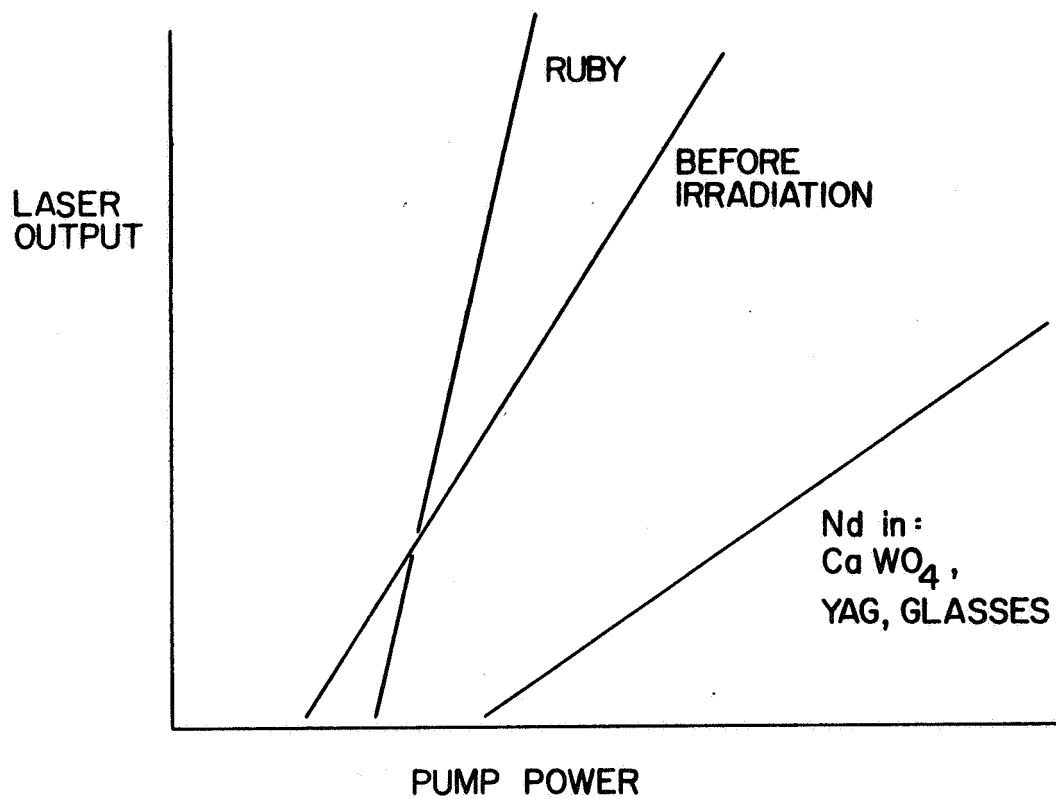
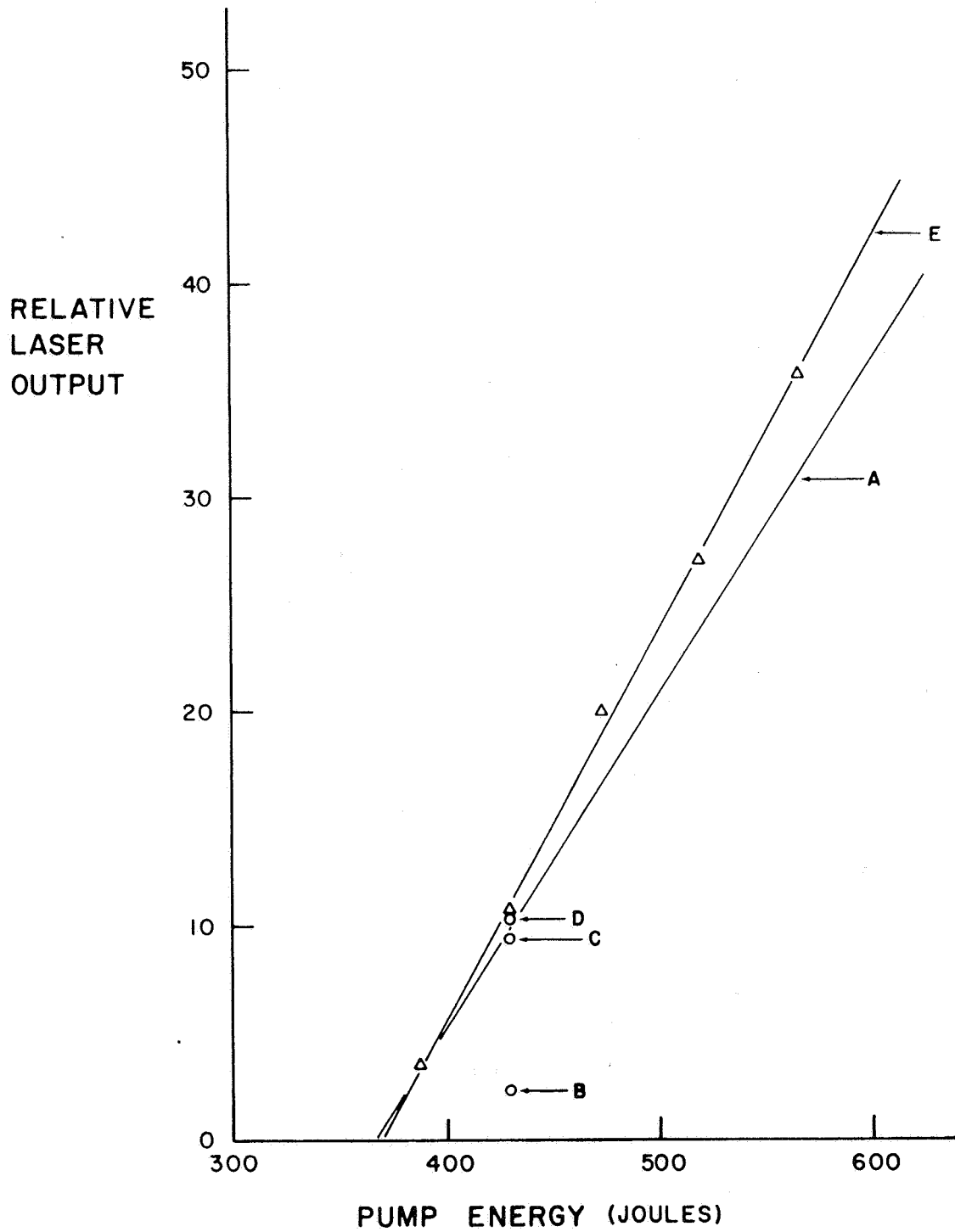Fig. 26--Effects produced in optically pumped lasers by irradiation

Fig. 27--Output of ruby laser vs pump energy before and after irradiation with 2.7×10^6 rads (gamma rays)

The ruby did not lase. A second flash at the same energy produced the point marked B, and the third and fourth flashes produced the points C and D. By this time, the orange color had nearly disappeared and subsequent flashes at different energies produced the line E. After a large number of flashes (~50) the laser again approached line A.

From our data on ruby, we conclude that two processes are involved. One increases the threshold (as for other types of optically pumped lasers), and the second enhances the efficient use of pump light. Both effects are optically bleached, but they probably do not arise from the same color center, since the first process appears to be optically bleached much more rapidly than the second. The second effect, enhancement, is associated with the orange color and we find that the absorption spectrum of carefully oriented ruby crystals shows enhanced optical density, after irradiation, at the wavelengths where the normal absorption due to Cr^{3+} occurs. A possible model may be that color centers increase the absorption constant of the Cr^{3+} in the crystal. The orange coloration is an ionization type of radiation effect; this was demonstrated by using 30 MeV electrons and gamma rays to color ruby samples. Equal doses of each type of radiation, expressed in rads, produced the same coloration, after the crystals were allowed to stand for two days to allow any room-temperature annealing to produce the same state in each crystal.

We conclude that the output of a ruby laser system will not be harmed by megarad doses of irradiation, if the laser is pumped often. Because of this, and because other workers have studied ruby[1, 2, 4, 30] no further measurements were made. It might, however, be desirable to study the effects of irradiation with 30 MeV protons, to find if this heavier particle leaves any residual damage effects which are not removed by optical bleaching.

3.4   Test of Model

The model[1] for the change produced by irradiation in the threshold and in the slope of the output-input curve was tested by comparing the changes in threshold and in slope. When the data showed little scatter, good agreement with the theoretical prediction was found. An example is shown in Fig. 28. Since the model predicts that the threshold, and the slope, will be changed by the factor $(1 + t_o/t_I)$, an irradiation will have more effect on an optimized laser, with low losses and a high t_o, than on a high-loss laser with a low t_o. It was planned to test this prediction, and thus the
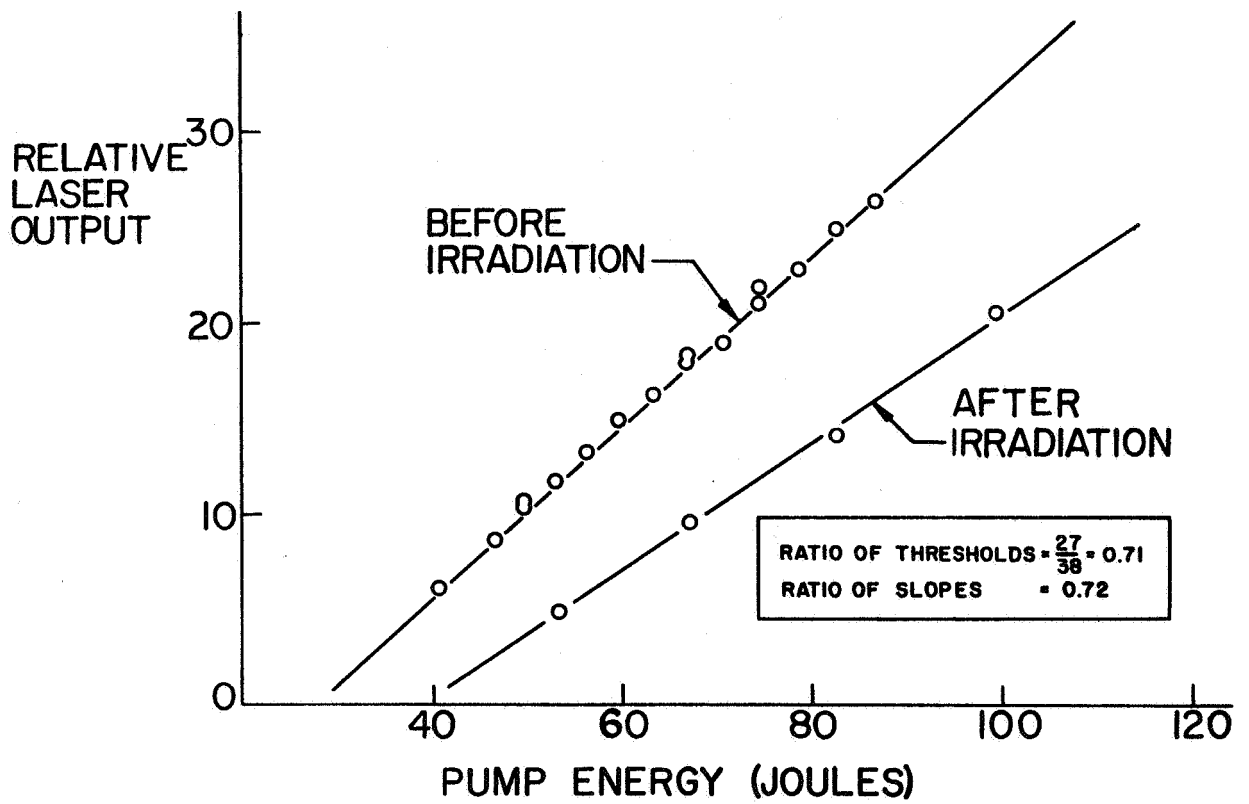
Fig. 28--Output of YAG: Nd laser vs pump energy before and after proton
irradiation, showing that the threshold energy is increased by
the same factor as the slope is decreased

model, by changing t_o by varying the reflectivity of the external mirrors in the optical cavity, and a set of mirrors with reflectivities of 98% to 70% was ordered for this purpose. However, the vendor had difficulty in meeting specifications and delivery was only made as this report was being completed.

3.5 Comparative Effects Due to Radiation Type and Laser Host; Importance of Spontaneous Annealing

Measurements of the effects of 30 MeV protons, 30 MeV electrons and fission-product gamma rays were made on Nd-doped lasers using each of the three host materials, $CaWO_4$, glass, and YAG. However, the relative effectiveness of different types of radiation and the relative susceptibilities to damage of the different types of lasers are not quantities that are simple to specify. This is because there is, in all cases, rapid and nearly complete spontaneous annealing of the radiation damage at $300^{\circ}K$. While this phenomenon complicates the measurements, it also means that these lasers are unlikely to be affected by any moderate exposure to space radiation at a temperature of $300^{\circ}K$.

The conclusions from our data are:

1. the three materials are each affected to a different extent by a radiation dose,

2. each material exhibits a different spontaneous recovery rate from the damage caused by a short exposure to radiation, and also shows different amounts of damage remaining after a long time (several days) has elapsed since irradiation,

3. to first order, the different types of radiation produce effects according to the dose they deliver in rads, i.e., the radiation effects are of ionization type, although there are some indications that proton damage leaves more residual effects than the other types of radiation, and

4. at low dose-rates of radiation (100 rad/hr), no effects are seen, up to 10^4 rads. Presumably the spontaneous annealing is rapid enough to keep the net damage to an undetectably low level.

53

The effect of radiation on a particular laser material will involve factors (1) and (2) and will thus depend on the time history of the irradiation and measurement.

The relative sensitivities of the different materials were determined by assembling the laser cavity at the General Atomic Linear Accelerator (Linac) and using the Linac to deliver a dose of ionizing radiation to the laser. The laser parameters can then be measured within a few seconds after irradiation. The changes in laser threshold obtained in this way before and 30 seconds after a dose of 1×10^{13} 30 MeV electrons/cm^2 are shown in Table I.

Table I

CHANGES IN LASER THRESHOLD DUE TO IRRADIATION

Material	$CaWO_4$:Nd	YAG:Nd	Glass:Nd
Initial Threshold (Joules)	33.0	72.0	60.0
Threshold 30 Seconds After Irradiation (Joules)	76.0	108.0	79.0
Ratio	2.3	1.5	1.3

The relative susceptibility is seen to be $CaWO_4$:Nd > YAG:Nd > Glass:Nd, at least for the particular rods used here, with their particular values of t_o. The same rods were examined using irradiation with 30 MeV protons from the USC proton linear accelerator. The rods were irradiated with 5×10^{10} 30 MeV protons/cm^2, which took 200 seconds, and then cooled to liquid nitrogen temperature after a further 100 seconds. On returning to General Atomic, the rods were warmed to 300^oK and their laser parameters were measured after another 300 seconds. The laser thresholds before and after irradiation are shown in Table II.

The $CaWO_4$:Nd is again the most affected, but by a smaller margin than in the experiment using electron irradiation. This presumably reflects the loss of some of the damage, with $CaWO_4$:Nd having the highest loss rate (see next page).

54

Table II

PRE- AND POST-IRRADIATION LASER THRESHOLDS

Material	$CaWO_4$:Nd	YAG:Nd	Glass:Nd
Initial Threshold (Joules)	12.0	28.0	68.0
Threshold After Irradiation (Joules)	20.0	45.0	95.0
Ratio	1.7	1.6	1.4

The recovery at short times after a short-duration radiation exposure was also measured using the electron Linac. No analytical model for the recovery could be found to fit the results, which are thus shown in a form found to be convenient, with the output at constant power plotted as a function of log time. Fig. 29 shows a plot of this type for $CaWO_4$:Nd, Fig. 30 for glass:Nd and Fig. 31 for YAG:Nd. $CaWO_4$:Nd shows a considerably faster recovery, with the other two showing similar recovery behavior.

The completeness of recovery from a radiation dose was determined by measuring the output-input curve before irradiation and again about two days after irradiation. This procedure was followed for all three types of laser, using gamma rays and protons, as examples of radiation types expected to show simple and more complex damage, respectively. For gamma rays, all three materials returned to the pre-irradiation condition within two days of a dose of 2.7×10^6 rads. One YAG:Nd rod that did not, was found to have suffered damage to its end mirrors from pitting, and thus suffered a permanent lowering in output. After a proton irradiation, of 4.6×10^{10} 30 MeV protons/cm^2, complete recovery after two days at 300°K was shown by $CaWO_4$:Nd, but appreciable residual damage was shown by glass:Nd and YAG:Nd. The glass:Nd showed a threshold shift from 68 to 73 joules and the YAG:Nd from 28 to 31 joules. Thermal annealing is moderately effective in removing radiation damage in these materials; annealing at 100°C for twenty-four hours lowered the threshold for the

Fig. 29--Recovery of output of $CaWO_4$:Nd laser at constant input power, after dose of 1×10^{13} 30 MeV electrons/cm^2

Fig. 30--Recovery of output of glass:Nd laser at constant input power, after dose of 1×10^{13} 30 MeV electrons/cm^2
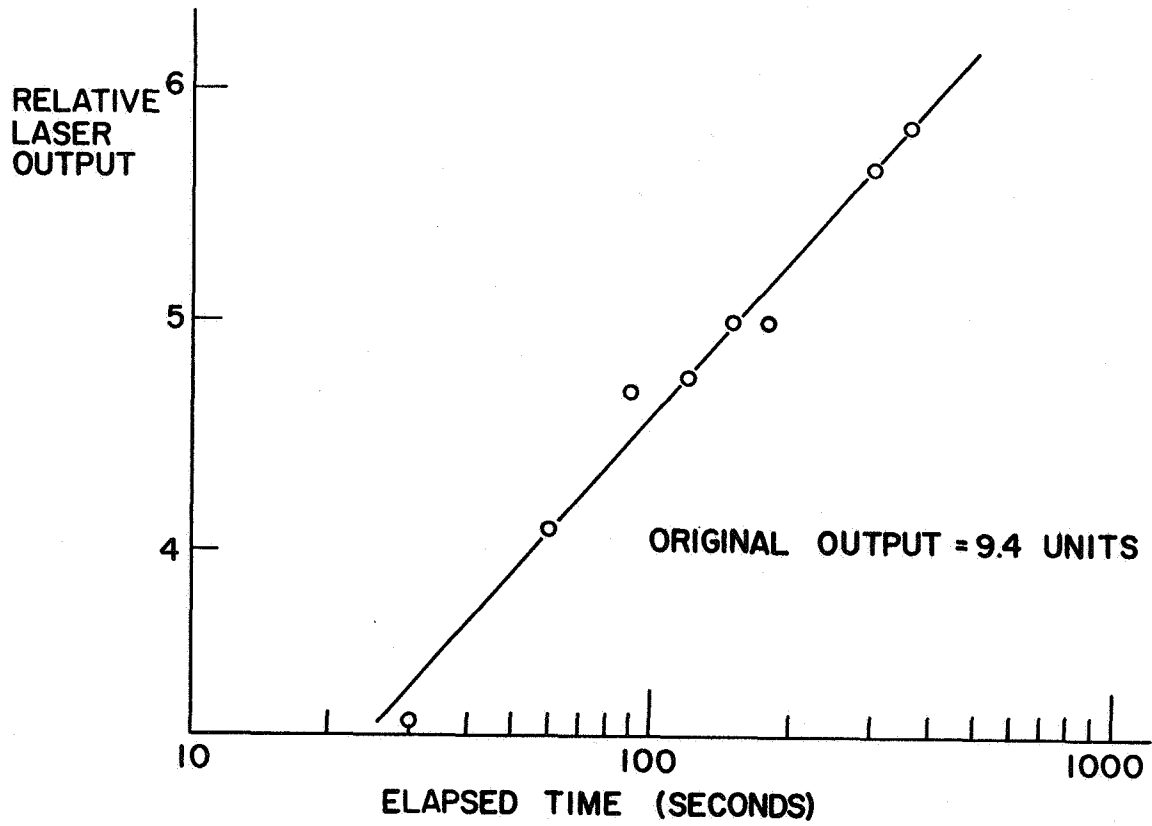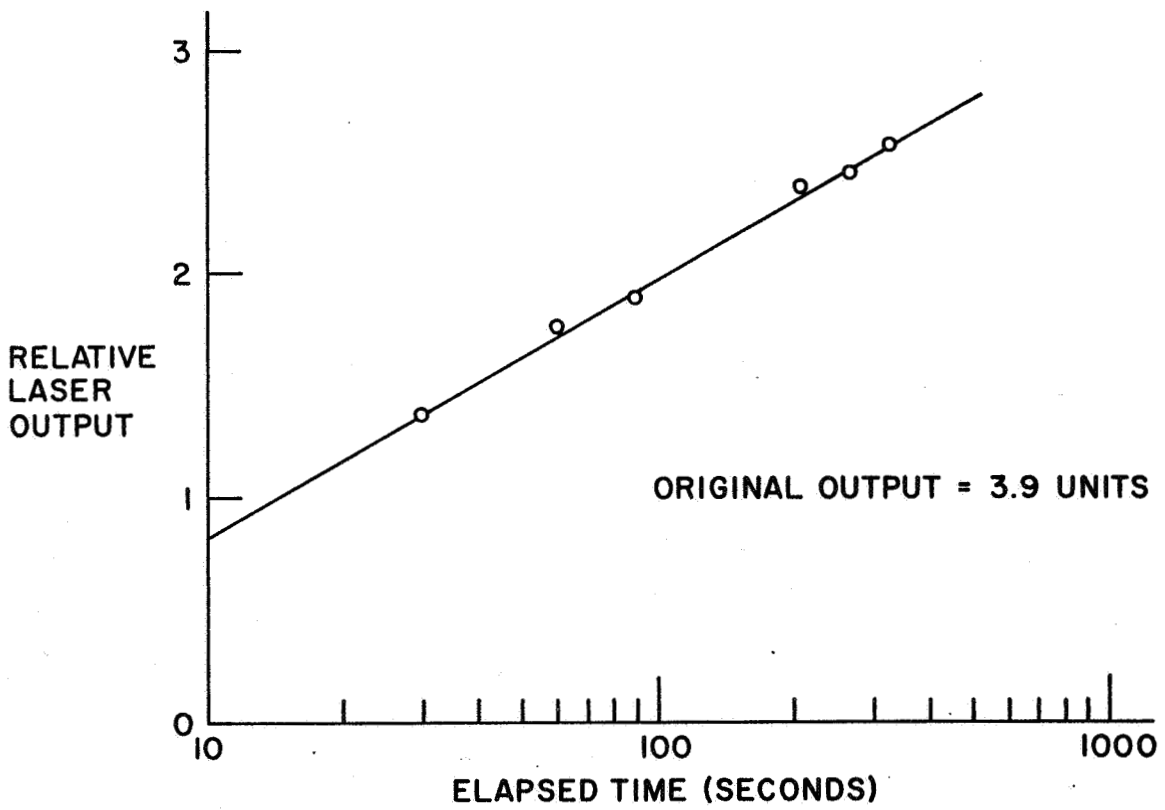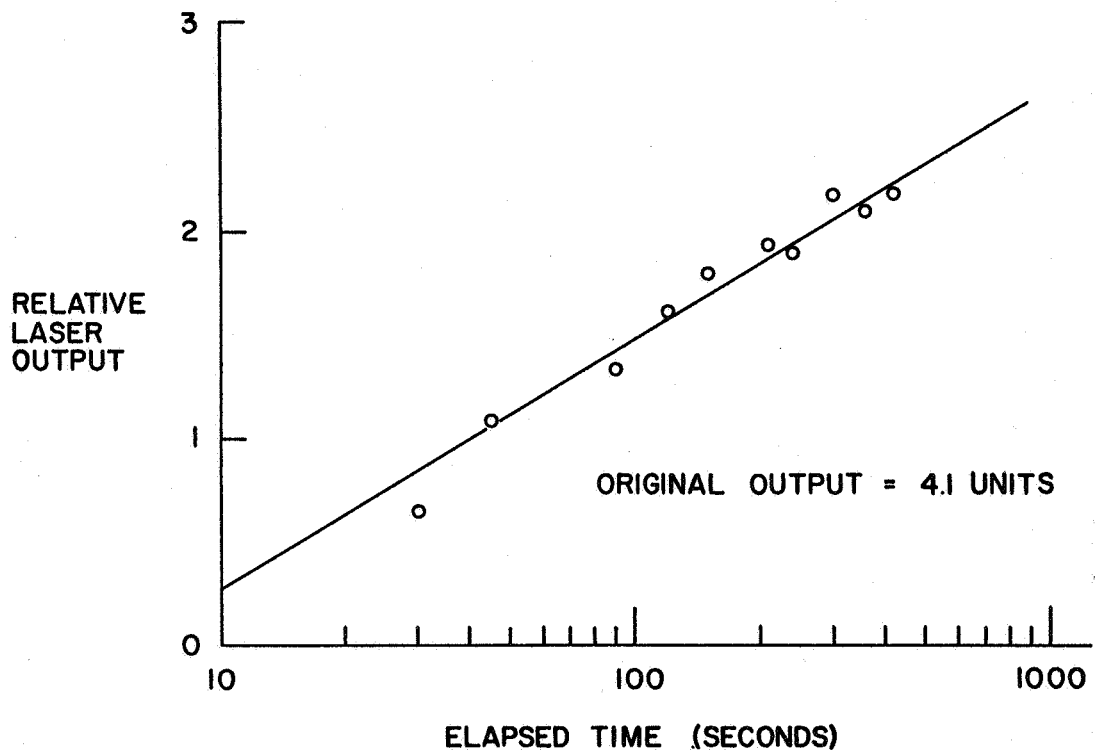
Fig. 31--Recovery of output of YAG:Nd laser at constant input power, after dose of 1×10^{13} 30 MeV electrons/cm^2

glass:Nd rod to 71 joules. Optical bleaching does not appear to be effective. Repeated flashlamp pulses have some effect in removing radiation damage, but this is chiefly a thermal effect. An anomalous effect is found with YAG:Nd where a moderate increase of temperature, near room temperature, due to heating by the flashlamp, causes an increase in laser output that was at one time thought to be an optical bleaching effect. However, it disappears on cooling. No optical bleaching is produced by laser emission light. This was shown by placing a radiation-damaged rod in the two rod cavity of Fig. 25 and pumping the second (other) laser rod. No reduction in the damage in the first rod was measurable.

3.6 Conclusions and Recommendations

1. The model previously developed to relate radiation-induced changes in threshold to changes in slope appears to give a satisfactory description of the behavior of $CaWO_4$:Nd, YAG:Nd and glass:Nd.

2. The effects of 30 MeV electrons, 30 MeV protons and (~ 0.7 MeV) gamma rays are nearly equivalent, when expressed in terms of energy deposition, i.e., the effects are of ionization type.

3. The optically pumped lasers examined show very rapid recovery at 300°K from radiation damage. There are slight residual effects from proton bombardment, but these are small. The low dose rates and doses to be expected in all but the most severe space environments are thus not likely to affect their performance at 300°K.

4. Some further work should be performed to relate the optical loss due to damage to that already present in the laser system. The potential damage to a completely optimized laser system, which is expected to be relatively more severe than to the "lossy" systems examined here, can then be evaluated. Further work on neutron damage, which is not expected to show fast recovery, is also needed. Measurements at low temperatures would be needed if the laser has to be operated below 300°K.

IV

PHOTODETECTORS

Since photodetectors form an essential part of a laser system, a start has been made on measuring the effects of radiation on these devices.

Relatively little work has been done on radiation damage to infrared detectors, although there is, of course, a vast body of literature on solar cells, both Si and GaAs. In a recent review appearing in the Naval Ordnance Laboratory Photodetector Series by Dewaard,[31] the author concluded that there are serious omissions in the available data, particularly with regard to the types of radiation to be expected in the trapped radiation belts. Such infrared detectors as have been studied are generally outdated types and these have been irradiated chiefly with neutrons and γ-rays. Results up to 1959 were summarized by Kutzscher.[32] A report prepared for the Navy[33] on gamma, electron, and neutron bombardment of PbS, PbSe, and Si photodetectors concluded that radiation-induced chemical reactions on the surfaces of the devices were the chief cause of the degradation observed. Proton damage effects on PbS infrared detectors were reported by Billups and Gardner.[34] Neutron and gamma irradiation studies of Ge/Hg and Ge/Cu infrared detectors using a nuclear reactor were made by Martzin, et al.[35] They found a marked decrease in detectivity after irradiation; this was not due to a change in responsivity (see below), but rather to a decrease in the conductivity of these photo-conductive devices.

A flux of ionizing radiation will also produce a spurious signal (or enhanced noise) in infrared photodetectors. Large effects of this kind produced by pulsed irradiation are discussed in a report by van Lint et al.,[36] and excess noise derived from gamma irradiation is discussed by Martzin et al.[35], and by Kutzscher[32]. The effect is only appreciable at >100 rads/hr and is thus negligible at the dose rates encountered in most space environments. Special apparatus has been acquired and set up to make measurements on infrared photodetectors, and the first measurements have been made on a photovoltaic device, the Texas Instruments IAV 6101. This is a single-crystal indium arsenide cell, having a peak response at 3 to 3.5 μ. It was chosen for a first study since it is a reasonably well-behaved detector, has high sensitivity, is of single crystal construction, and is moderately priced.

4.1 Terminology and Typical Performance

The testing and evaluation of the photodetectors relied upon conventional terminology and procedures used by the manufacturers. Two main quantities are important, the responsivity to infrared energy, and the noise. These are usually combined into a figure of merit, D^*, the detectivity. Since this varies with measuring conditions, which generally chop the infrared radiation and use synchronous detection to improve signal/noise, D^* is identified as $D^*(\lambda, f, \Delta f)$, where λ is the wavelength of infrared light being used, f is the frequency at which the infrared light is chopped and the signal detected, and Δf is the bandwidth equivalent of the detection circuit. Typical testing conditions yield a D^* characterized by $D^*(\lambda, 1000, 1)$, i.e., chopping infrared light of wavelength λ at 1000 Hz and detecting the signal with an equivalent bandwidth of 1 Hz at 1000 Hz, or by $D^*(500, 1000, 1)$ where the first term refers to a 500°K blackbody source used to supply infrared radiation.

D^* combines signal and noise according to the relation

$$D^* = \frac{S}{NJ} \left[\frac{\Delta f}{A}\right]^{\frac{1}{2}} , \qquad (6)$$

where S is the signal (RMS volts) from the detector when exposed to the source; N the noise (RMS volts) when the detector is exposed only to a 300°K environment, the noise being measured in a narrow bandwidth Δf centered at the chopping frequency. A is the sensitive area of the detector (cm^2) and J is the RMS flux density (watts cm^{-2}) incident on the detector. The relation may be used to compute a standardized value of D^* from data taken at particular values of J, A, and Δf. Another useful term is responsivity (R), where R = S/J (volts $cm^2/watt^{-1}$).

For the indium arsenide photovoltaic detectors, the manufacturer gives the curve of relative noise voltage vs chopping frequency shown in Fig. 32A. The noise voltage is essentially constant at frequencies of 500 Hz and above. Thus, any chopping frequency above 500 Hz is satisfactory and will give results equivalent to those at 1000 Hz. Since a 510 Hz chopper was available, this frequency was used in our measurements. (Texas Instruments uses 450 Hz to make most of its detector calibrations).
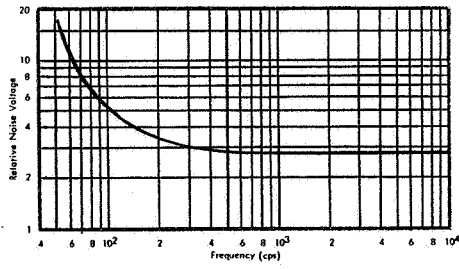
Figure IAV-10   Relative Noise Voltage
versus Frequency. Relative Noise Spectra
are Essentially Constant with Temperature

A

Figure IAV-13 DC Short Circuit
Impedance for InAs

B

Figure IAV-11   AC Open Circuit Noise
Voltage versus Temperature for InAs
at DC Short Circuit

C
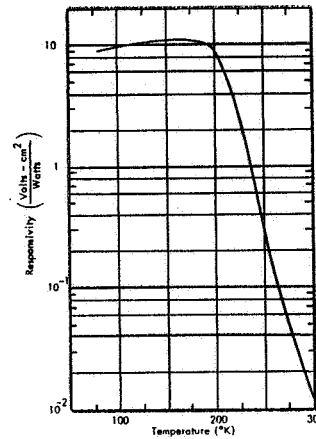
Figure IAV-12   500 K Blackbody
Responsivity versus Temperature for InAs
at DC Short Circuit and AC Open Circuit

D

Figure IAV-6   Blackbody Detectivity
at Several Temperatures

E

Fig. 32--Manufacturer-supplied curves for typical performance of the
InAs detector.   Parameters as shown.   Curves copied from
brochure of Texas Instruments Inc., Dallas, Texas

62

The characteristics of the detector change rapidly with temperature. The diode impedance vs temperature is shown in Fig. 32B, and falls rapidly above 200°K. This leads to an AC open circuit noise voltage (Fig. 32C) that is nearly constant up to 175°K and then falls. The responsivity falls very rapidly above 200°K (Fig. 32D), leading to a D^* that is nearly constant up to 200°K and then falls rapidly (Fig. 32E). Measurements at both 77°K and 300°K thus appear to be needed for the study of radiation effects. A cryostat was built that allowed the diode to be maintained at temperatures between 77°K and 300°K, and provided adequate shielding against rf pickup, which was found in early measurements to be a source of excess noise.

4.2   Measurement Technique

For simplicity, ac open-circuit, dc short-circuit operation was chosen. The diode is connected to a transformer which is connected to a low-noise preamplifier. The overall system is shown in Fig. 33. The radiant flux is provided by a 500°K blackbody source. This is a Barnes Engineering, Model 11-110T, with aperture plate, and provides a radiant flux of 0.1128 watt cm^{-2} steradian^{-1}. The 300°K aperture plate enables the emitting area to be reduced in a succession of steps of three. The flux is chopped by a wheel at 300°K, at a frequency of 510 Hz. The photodiode is mounted in a cryostat. A Triad Geoformer with an input impedance of 30 Ω and an output impedance of 157,000 Ω, Model G4, is used to couple the diode to the preamplifier, a Tektronix type 122, set to a bandpass of 80 Hz to 10 K Hz, with a gain of 10^3. The tuned voltmeter used is a Hewlett-Packard, Model 302 wave analyzer, set to 510 Hz, with a bandpass of 6 Hz. The output of the wave analyzer is passed through an RC integrator with a time constant of 10 or 100 seconds, to a recorder. The RC integrator smooths the dc output of the wave analyzer, but does not affect the effective bandwidth. The system is calibrated with an oscillator and calibrated attenuator.

With this arrangement the noise voltage was measured with the diode in place (N_1) and with the input to the transformer shorted (N_2); N, the noise voltage output of the diode was then taken as $N = \sqrt{N_1^2 - N_2^2}$, and corrected from $\Delta f = 6$ Hz to $\Delta f = 1$ Hz by multiplying by $\sqrt{6}$. The noise voltage measured at 300°K was in good agreement with that reported by the manufacturer for 300°K, e.g., 4.90×10^{-10} volts as compared to 4.95×10^{-10} volts.
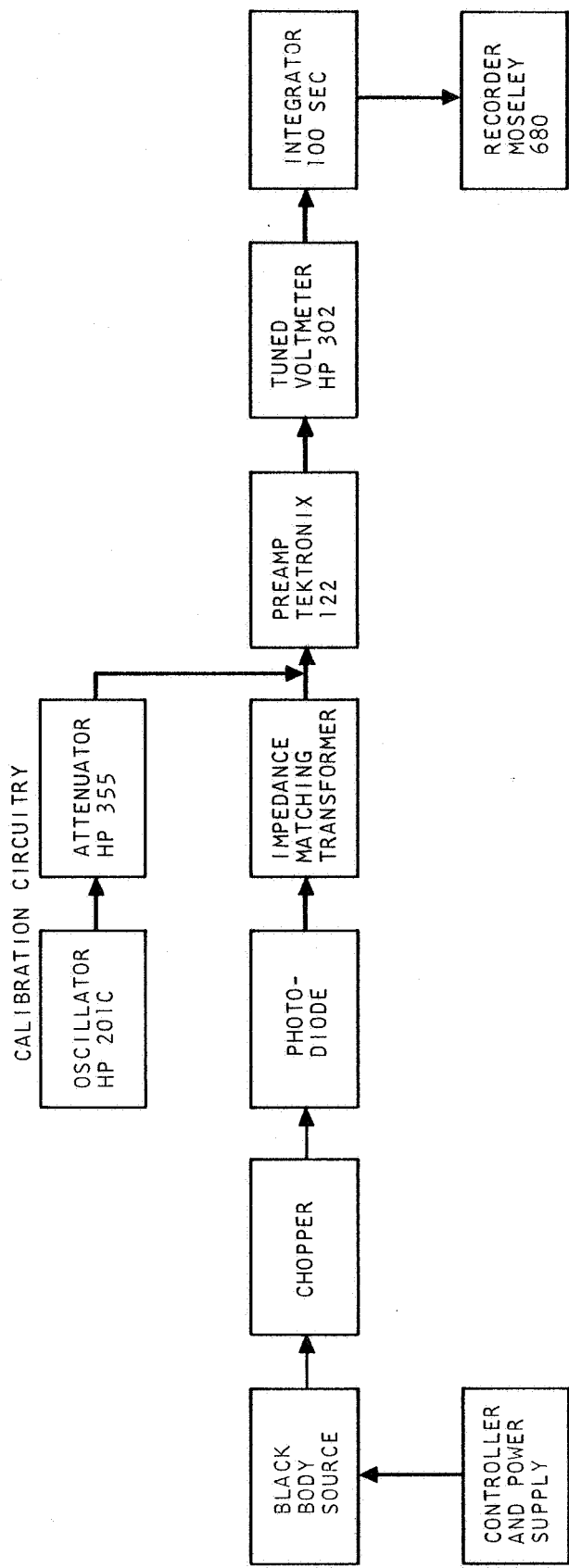
Fig. 33--Block diagram of system used to measure noise and responsivity

CALIBRATION CIRCUITRY

OSCILLATOR HP 201C

ATTENUATOR HP 355

PREAMP TEKTRONIX 122

TUNED VOLTMETER HP 302

INTEGRATOR 100 SEC

RECORDER MOSELEY 680

BLACK BODY SOURCE

CHOPPER

PHOTO-DIODE

IMPEDANCE MATCHING TRANSFORMER

CONTROLLER AND POWER SUPPLY

The responsivity was determined at 77° and at 300°K, using the blackbody source. An experimentally determined correction factor is used to convert the chopped (square wave) input from the blackbody to an RMS value. If the chopped input were an exact square wave, the factor would be $\sqrt{2}/\pi$. The values found were in reasonably good agreement with those reported by the manufacturer, e.g., 8×10^{-3} volts cm^2 watt^{-1} as compared to 7.4×10^{-3} volts cm^2 watt^{-1}. The output is linear with input flux (determined using the aperture plate) as is expected for the dc-shorted mode of operation. The speed of response of the photodiode (0.5 μsec at 300°K) is measured by using a GaAs laser as light source. An InAs light-emitting diode can also be used.

4.3 Effects of Radiation

After calibration in this way, an InAs diode was given a series of irradiations at 300°K with 30 MeV electrons. After each irradiation, the noise and responsivity were remeasured at 300°K. The results of the noise measurements are shown in Fig. 34. There is a slight decrease in noise voltage with irradiation, but it is not clear whether this is due to a decrease in noise power, or whether the noise power remains constant, or even increases, and the change is due to a change in the impedance of the device. At present, no reliable measurements of impedance, under working conditions, have been made. Figure 35 shows the responsivity of the diode after each irradiation. There is a marked decrease with increasing dose, a decrease by approximately an order of magnitude being found for a dose of $\sim 1 \times 10^{13}$ 30 MeV electrons cm^{-2}. At least for electrons of this energy, the decrease of responsivity of the InAs diode is greater than the decrease in the output of a typically operated GaAs laser diode exposed to the same dose.

A model for the functional variation of the decrease of responsivity with dose has not yet been developed. If the responsivity were proportional to minority carrier diffusion length, which, in turn, is proportional to (lifetime)$^{\frac{1}{2}}$, a linear decrease of lifetime with irradiation dose would lead to a decrease of responsivity with dose according to an equation of the form

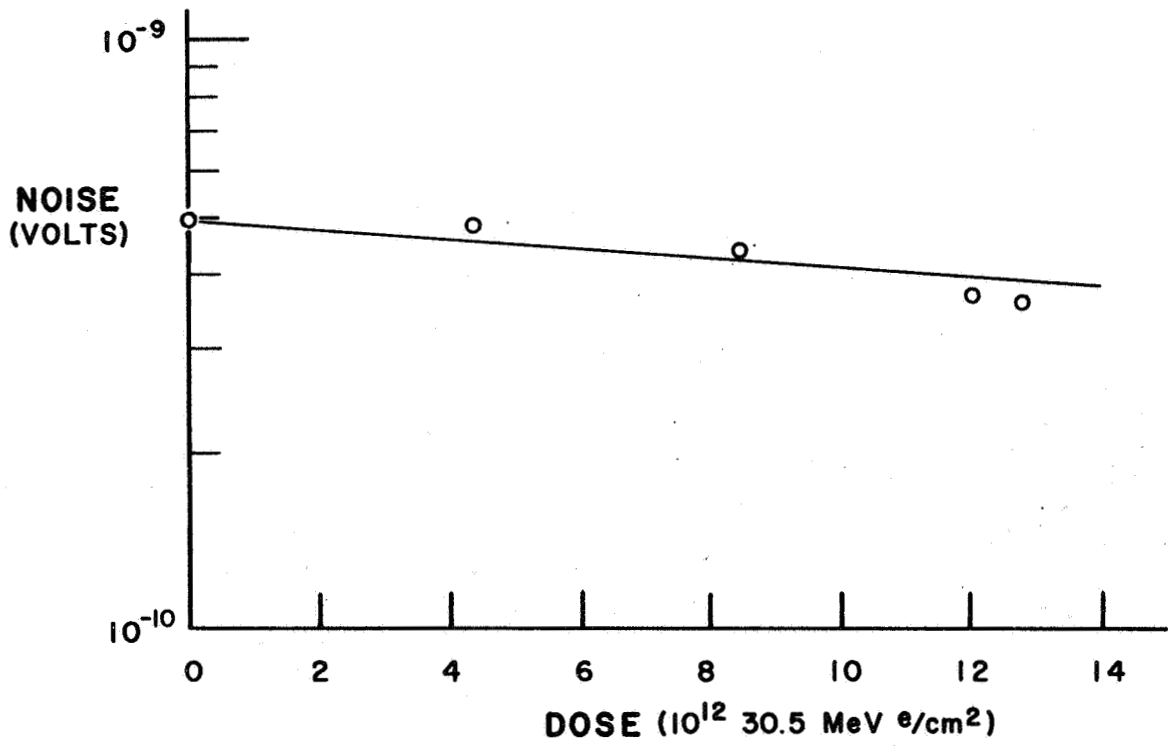$$\left[\frac{R_o^2}{R_i^2}\right] - 1 \propto dose \quad , \tag{7}$$

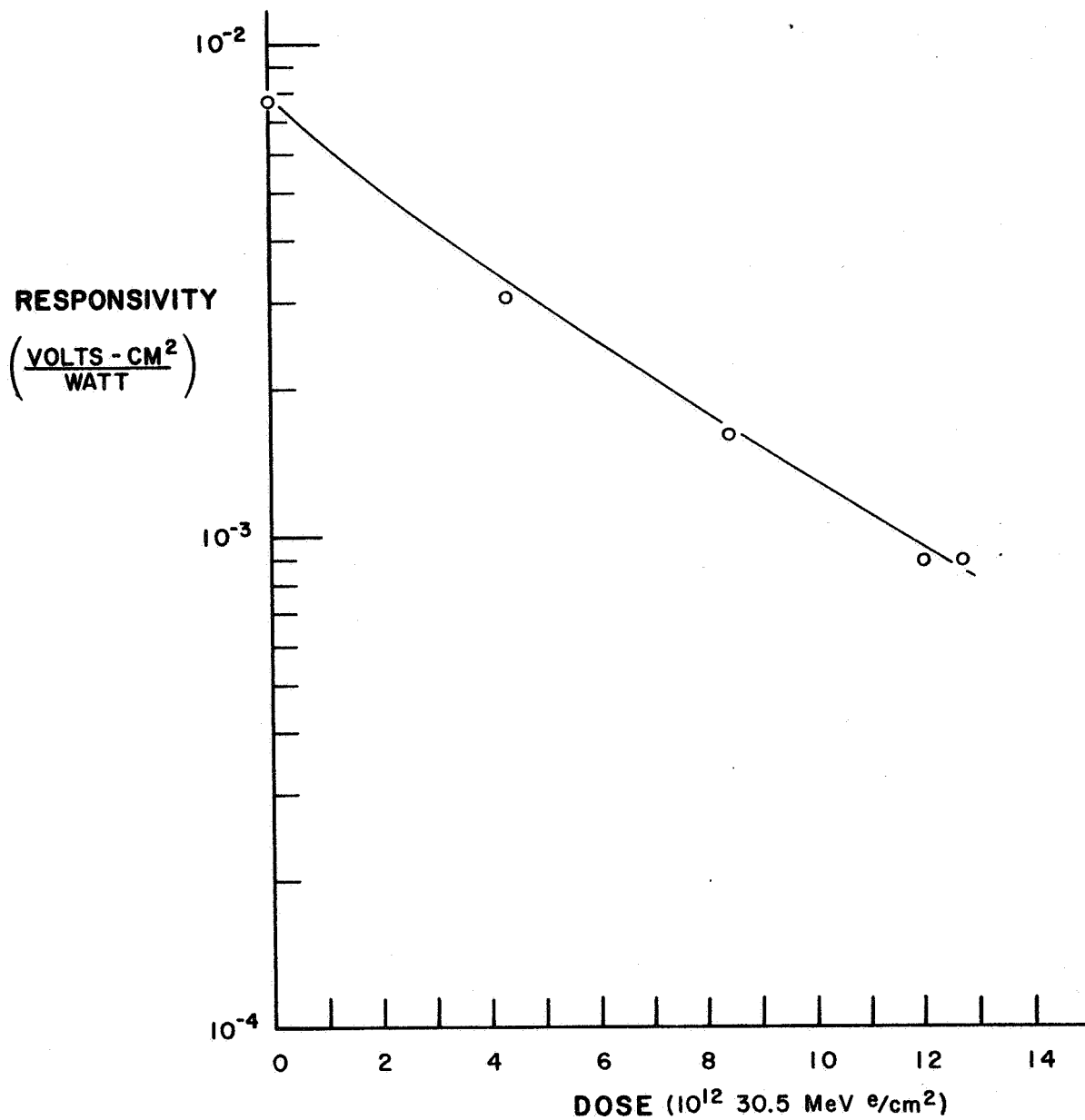Fig. 34--Noise voltage of InAs photovoltaic diode vs dose of 30 MeV
electrons

Fig. 35--Responsivity of InAs photovoltaic diode vs dose of 30 MeV
electrons

where R_0 is the initial responsivity and R_i that after irradiation. This is not observed. A satisfactory model will have to take into account the various depths at which carriers are formed, and the role of diffusion to the front surface and recombination there. Similar difficulties have been encountered in developing a theory for radiation damage to Si solar cells[37] and GaAs solar cells[38]. More experimental results are needed before it is worthwhile to formulate a more detailed theory. It is clear, however, that if radiation damage affects chiefly the lifetime in the layers near the front surface, and the surface recombination velocity, that low-energy particles may have an anomalously high importance, and careful measurements should be made with low-energy electrons and protons.

One useful experiment is to use the linear accelerator both for radiation damage, and to give short (10 nsec) pulses that can be used to measure the decay time of the photovoltaic signal. This decay time can be related to carrier lifetime, and thus the decrease of lifetime with dose can be measured and compared with the decrease of responsivity.

4.4   Annealing

An attempt was made to anneal the InAs diode by heating at 100°C for two hours. This procedure produced no recovery of the responsivity.

4.5   Conclusions and Recommendations

The preliminary results reported here show that

1.   techniques have been developed to make consistent and accurate measurements of the parameters of infrared detectors,

2.   InAs photovoltaic diodes, selected for a first test, show a large degradation in responsivity and a very slight decrease in noise voltage on irradiation with 30 MeV electrons, giving a large degradation in detectivity, and

3.   measurements with other energies and types of radiation need to be made and a satisfactory model for the radiation damage is yet to be developed.

REFERENCES

1. D.M.J. Compton and R. A. Cesena, "Radiation Effects on Lasers," National Aeronautics and Space Administration Report GA-7274, September, 1966.

2. V.R. Johnson and R.W. Grow, IEEE Journal of Quantum Electronics QE3, 1 (1967).

3. V.R. Johnson and R.W. Grow, Proc. IEEE 52, (1964).

4. A.F. Forestieri and H.H. Grimes, "Effect of Ionizing Radiation on Ruby," NASA Report, NASA-TN-D-3379, April, 1966.

5. M. Saji and Y. Inuishi, Japan J. Appl. Phys. 4, 830 (1965).

6. J.H. Doede, et al., Z. Angew. Math. Phys. (Switzerland) 16, 99 (1965); abstract of paper given at Laser Physics and Applications Symposium, Bern (1964).

7. M.C. Petree, Appl. Phys. Letters 3, 67 (1963).

8. M.F. Millea and L.W. Aukerman, Appl. Phys. Letters 5, 168 (1964).

9. L.W. Aukerman and M.F. Millea, J. Appl. Phys. 36, 2585 (1965).

10. M.F. Millea and L.W. Aukerman, J. Appl. Phys. 37, 1788 (1966).

11. L.W. Aukerman, M.F. Millea and M. McColl, J. Appl. Phys. 38, 685 (1967).

12. L.W. Aukerman, M.F. Millea and M. McColl, IEEE Trans. Nucl. Sci. NS-13,174 (1966).

13. L.W. Aukerman and R.D. Graft, Phys. Rev. 127, 1576 (1962).

14. L.W. Aukerman, et al., J. Appl. Phys 34, 3590 (1963).

15.   R. Bauerlein, Z. Physik 176, 498 (1963).

16.   J. A. Grimshaw and P.C. Banbury, Proc. Phys. Soc. (London)
        84, 151 (1964).

17.   J.J. Loferski and M.H. Wu, "Studies of Radiation Defects in GaAs
        Based on Proton- and Electron-Bombardment Induced Light
        Emission," in Radiation Damage in Semiconductors, Paris,
        Dunod (1965).

18.   J.L. McNichols and W.S. Ginell, J. Appl. Phys. 38, 656 (1967).

19.   M. Nathan, Proc. IEEE 54, 1276 (1966).

20.   L.E. Glendenin, Nucleonics 2, No. 1, 12 (1948).

21.   A. Sosin, Phys. Rev. 126, 1698 (1962).

22.   G.W. Arnold, Phys. Rev. 149, 679 (1966).

23.   D.P. Cooper, C.H. Gooch, and R.J. Sherwell, IEEE, J. Quantum
        Elect. QE-2, 329 (1966).

24.   M.E. Wyatt, V.A.J. van Lint, and E.G. Wikner," Proton Correla-
        tion Studies," Air Force Weapons Laboratory Report AFML-TR-
        66-77, April 1966 (AD486-487).

25.   G. Burns and M.I. Nathan, Proc. IEEE 52, 770 (1964).

26.   A.W. Smith and J.A. Armstrong, IBM Journal 10, 225 (1966).

27.   M.F. Lamorte and T. Gonda, IEEE J. Quantum Elect. QE-2, 9
        (1966).

28.   M.I. Nathan, A.B. Fowler, and G. Burns, Phys. Rev. Letters,
        11, 152 (1963).

29.   M.H. Pilkuhn and H. Rupprecht, J. Appl. Phys. 38, 5 (1967);
        ibid., R.O. Carlson, 38, 661 (1967).

30. J. J. Halpin and R. Wensel, U. S. Naval Research Laboratory, Washington, D. C. Private communication.

31. R. DeWaard, "Nuclear Radiation Effects on Infrared Detectors and Optical Materials," in Properties of Photodetectors, N. O. L.C. Report 637 (AD 631225), by W. L. Eisenman, Naval Ordnance Laboratory, Corona, California, February 15, 1966.

32. E. W. Kutzscher, Proc. IRE 47, 1520 (1959).

33. D. E. Martz and I. R. Neilsen, "Final Report on the Effects of Ionizing Radiation on Photodetectors," Navy Contract N 123(60530) 26834A, February, 1963.

34. R. R. Billups and W. L. Gardner, Proc. IRIS 6, 69 (1961) and Infrared Physics 1, 199 (1961).

35. G. Martzin, D. Brown, and J. P. Walker, Jr., Proc. IRIS 10, 9 (1965).

36. V. A. J. van Lint, et al., "Effect of Pulsed Gamma Radiation on Infrared Detectors," Air Force Special Weapons Command Report SWC-TDR-62-29, May 1962 (AD 283368).

37. J. A. Baicker and B. W. Faughnan, J. Appl. Phys. 33, 327 (1962).

38. J. J. Wysocki, J. Appl. Phys. 34, 2915 (1963).